2

Qualitative theory of non-smooth dynamical systems

In this chapter, we give an overview of the basic theory of both smooth and non-smooth dynamical systems, to be expanded upon in later chapters. In particular we shall define what we meant by each of the *italicized terms* encountered in Chapter 1. We start with the definition of a dynamical system and review the essential concepts from the theory of smooth dynamical systems that can also apply to non-smooth systems. This material is available in the now many textbooks on nonlinear dynamics and chaos, and so only the briefest of details are given, with appropriate references. Next, in Sec. 2.2, we define carefully what we mean by the different classes of piecewise-smooth dynamical systems that we treat. In Sec. 2.3, we point out the relation to some of the other mathematical formalisms that exist for defining non-smooth systems. Section 2.4 considers notions of stability and bifurcation in non-smooth systems and introduces the key concept of the book, that of *discontinuity-induced bifurcation* (DIB), where an invariant set changes its topology with respect to the set of discontinuity surfaces. This is naturally followed by Sec. 2.5, which explains the idea of a *discontinuity mapping* (DM) which is the main analytical tool to be used in Chapters 6–8. The chapter ends with a brief discussion in Sec. 2.6 of numerical methods for simulation, parameter continuation and bifurcation detection in non-smooth systems.

2.1 Smooth dynamical systems

The qualitative theory of differential equations [7, 124, 273, 168] begins with a quite general definition of a dynamical system. This is written in terms of an n-dimensional state space (or phase space) $X \subset \mathbb{R}^n$ (with the usual topology) and an evolution operator ϕ that takes elements x_0 of the phase space and evolves them through a 'time' t to a state x_t

$$\phi^t : X \to X, \qquad x_t = \phi^t(x_0).$$

The time t takes values in an index set T, which we usually consider to be either discrete (the integers $\mathbb{Z}$) or continuous (the real numbers $\mathbb{R}$). Note that ϕ may not be uniquely defined for all $t \in T$. For example, so called *noninvertible* dynamical systems may not be defined for $t < 0$; or in certain systems, some initial states x_0 may diverge to infinity in a finite time. Formally, in these cases we need to define a space-dependent subset $T^*(X) \subset T$ such that $\phi^t(x)$ is uniquely defined for $x \in X$ provided $t \in T^*(X)$. We shall, however, ignore such technicalities, other than to state that only positive time should be taken for noninvertible systems.

Definition 2.1. *A state space X, index set T and evolution operator ϕ^t are said to define a* **dynamical system** *if*

$$\phi^0(x) = x, \quad \textit{for all} \quad x \in X, \tag{2.1}$$
$$\phi^{t+s}(x) = \phi^s(\phi^t(x)) \quad \textit{for all} \quad x \in X, \quad t, s \in T. \tag{2.2}$$

The set of all points $\phi^t(x)$ for all $t \in T$ is called the **trajectory** *or* **orbit** *through the point x.*

The **phase potrait** *of the dynamical system is the partitioning of the state space into orbits.*

Remarks

1. Properties (2.1) and (2.2) define ϕ^t to be a *semi-group.*
2. When the dynamical system is invertible (uniquely defined for $t < 0$ as well as for $t > 0$), then we have the additional property that is a consequence of (2.1) and (2.2)
$$\phi^t \phi^{-t} = \mathrm{id}.$$

Definition 2.2. *A dynamical system satisfying (2.1) and (2.2) is said to be* **smooth of index** *r, or C^r, if the first r derivatives of ϕ with respect to x exist and are continuous at every point $x \in X$.*

We shall often be interested in dynamics that is, in some sense, recurrent or repeatable. Specifically, we will gain an understanding of the phase space structure by from specific sets that remain invariant under the system dynamics.

Definition 2.3. *An* **invariant set** *of a dynamical system (2.1), (2.2) is a subset $\Lambda \subset X$ such that $x_0 \in \Lambda$ implies $\phi^t(x_0) \in \Lambda$ for all $t \in T$. An invariant set that is closed (contains its own boundary) and bounded is called an* **attractor** *if*

1. *for any sufficiently small neighborhood $U \subset X$ of Λ, there exists a neighborhood V of Λ such that $\phi^t(x) \in U$ for all $x \in V$ and all $t > 0$, and*
2. *for all $x \in U$, $\phi^t(x) \to \Lambda$ as $t \to \infty$.*

The set of all attractors of a given system typically describes the long-term observable dynamics. A given dynamical system may have many competing attractors, with their relative importance being indicated by the size of the set of initial conditions that they attract; that is, their *domain of attraction*

Definition 2.4. *The* **domain of attraction** *(also known as the basin of attraction) of an attractor Λ is the maximal set U for which $x \in U$ implies $\phi^t(x) \to \Lambda$ as $t \to \infty$.*

We already saw in Fig. 1.14(a) that domains of attraction in non-smooth systems can have remarkably complicated structures, which can be true in smooth systems too.

Another useful notion is to define points in phase space that are eventually approached infinitely often in the future, or were approached infinitely often in the past.

Definition 2.5. *A point p is an* **ω-limit point** *of a trajectory $\phi^t(x_0)$ if there exists a sequence of times $t_1 < t_2 < \ldots$ with $t_i \to \infty$ as $i \to \infty$ such that $\phi^{t_i}(x_0) \to p$ as $t_i \to \infty$. If instead there exists a sequence of times with $t_1 > t_2 > \ldots$ and $t_i \to -\infty$ and $\phi^{t_i}(x_0) \to p$, then we say that p is an* **α-limit point** *of x_0. The ω- (α-) limit set of x_0 is the set of all possible ω- (α-) limit points. The set of all such ω-limit points (or α-limit points) for all $x_0 \in X$ is called the* **ω-limit set** *(or* **α-limit set***) of the system. This set is closed and invariant.*

An ω-limit point is sometimes called a *recurrent point* of the dynamical system.

There is only so much that can be gained from this abstract definition of a dynamical system. Its usefulness is that it defines properties like attractors, and domains of attraction for quite general classes of system such as partial differential equations, systems with time delays and discrete-valued systems. However, when dealing with smooth systems, we shall largely only be interested in cases where the state space X is (possibly some subset of) Euclidean space $\mathbb{R}^n$ and the evolution is either described by a discrete-time map or a continuous-time flow. We now take each in turn.

2.1.1 Ordinary differential equations (flows)

Given a system of *ordinary differential equations* (ODEs)

$$\dot{x} = f(x), \quad x \in \mathcal{D} \subset \mathbb{R}^n, \tag{2.3}$$

where $\mathcal{D}$ is a domain, then $\{X, T, \phi^t\}$ defines a dynamical system if we set $X = \mathcal{D}$ and $T = \mathbb{R}$ and let $\phi^t(x) := \Phi(x, t)$ be the solution operator or *flow* that takes initial conditions x up to their solution at time t:

$$\frac{\partial}{\partial t}\Phi(x,t) = f(\Phi(x,t)), \qquad \Phi(x,0) = x\,. \tag{2.4}$$

Remarks

1. If we suppose the vector field f is C^{r-1} for some $r > 2$, then (2.4) implies the flow $\Phi(x,t)$ is one index smoother; that is, the dynamical system is C^r, since f is a derivative of Φ.
2. Note that we have not included in the above the possibility that the vector field f depends explicitly on time t. However such systems can be treated within the general framework by allowing time to be an additional dynamical state. For example, taking the $(n+1)$st state $x_{n+1} = t$, implies $\dot{x}_{n+1} = 1$ so that the $(n+1)$st component of f is unity. In many examples time appears periodically, and then it can be helpful to consider the phase space to be cylindrical:

Example 2.1 (A periodically forced system). Consider the forced system

$$\ddot{u} + 2\zeta\dot{u} + ku = a\cos(\omega t). \tag{2.5}$$

If we set $X = \mathbb{R}^2 \times S^1 \subset \mathbb{R}^3$, with $x_3 = t \bmod(2\pi/\omega)$, we obtain

$$\begin{aligned} \dot{x}_1 &= x_2, \\ \dot{x}_2 &= -kx_1 - 2\zeta x_2 + ax_3, \\ \dot{x}_3 &= 1, \end{aligned}$$

with corresponding phase potrait depicted in Fig. 2.1.

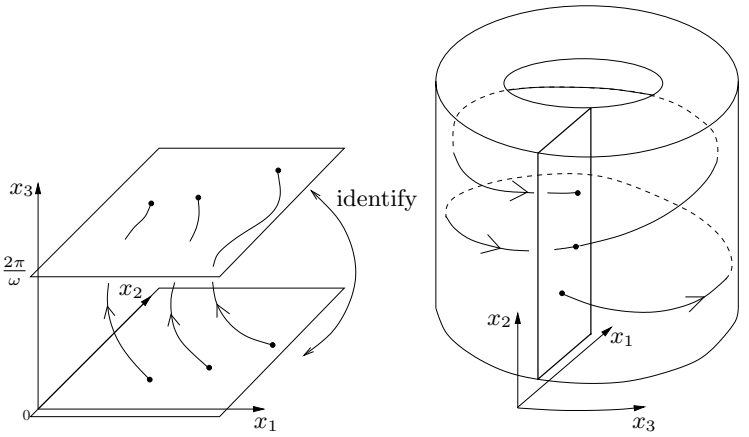

Fig. 2.1. Schematic description of the cylindrical phase space associated with the periodically forced system (2.5).

We shall be concerned with systems that depend on parameters. So we shall often write

$$\dot{x} = f(x, \mu),$$

where $\mu \in \mathbb{R}^p$ is a set of parameters. If we say that f is smooth, we mean that the dependence on μ is as smooth as it is on x. Unless it is crucial, we shall often drop the explicit parameter dependence of f and return to the more compact notation $f(x)$.

Systems of ODEs can exhibit the following kinds of invariant sets, see Fig. 2.2.

Equilibria. The simplest form of an invariant set of an ODE is an *equilibrium* solution x^* which satisfies $f(x^*) = 0$. These are also sometimes called *stationary points* of the flow since $\Phi(x^*, t) = \Phi(x^*, 0)$ for all t.

limit cycles. The next most complex kind of invariant set would be a *periodic orbit*, which is determined by an initial condition x_p and a period T. Here T is defined as the smallest time $T > 0$ for which $\Phi(x_p, T) = x_p$. periodic orbits form closed curves in phase space (topologically they are circular). A periodic orbit that is isolated (does not have any other periodic orbits in its neighborhood) is termed a *limit cycle*.

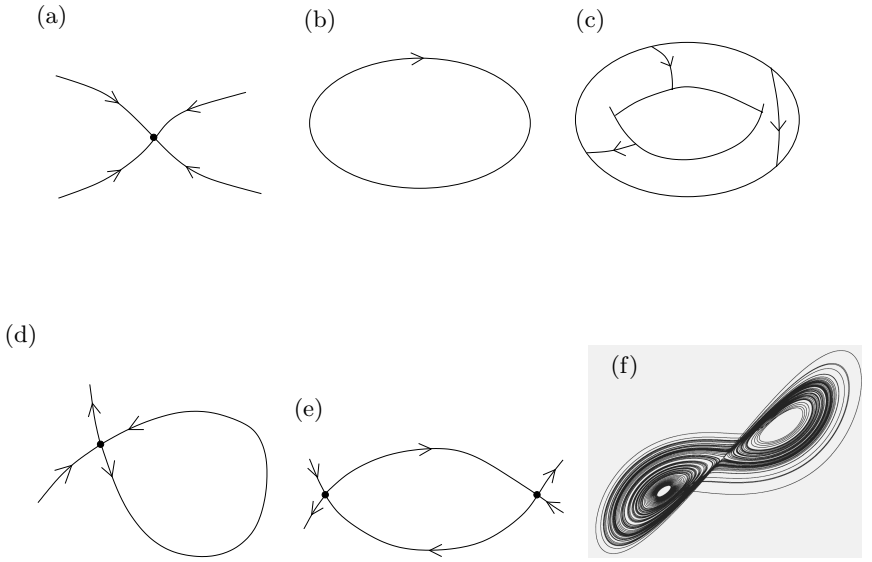

Fig. 2.2. Phase potrait representation of invariant sets of smooth flows: (a) equilibrium, (b) limit cycle, (c) invariant torus, (d) homoclinic orbit, (e) heteroclinic orbit, (f) chaotic attractor.

Invariant tori. Invariant tori are the nonlinear equivalent of two-frequency motion (see Fig. 2.3). Flow on a torus may be genuinely quasi-periodic in that it contains no periodic orbits, or it may be *phase locked* into containing a stable and an unstable periodic orbit, which wind a given number of times around the torus.

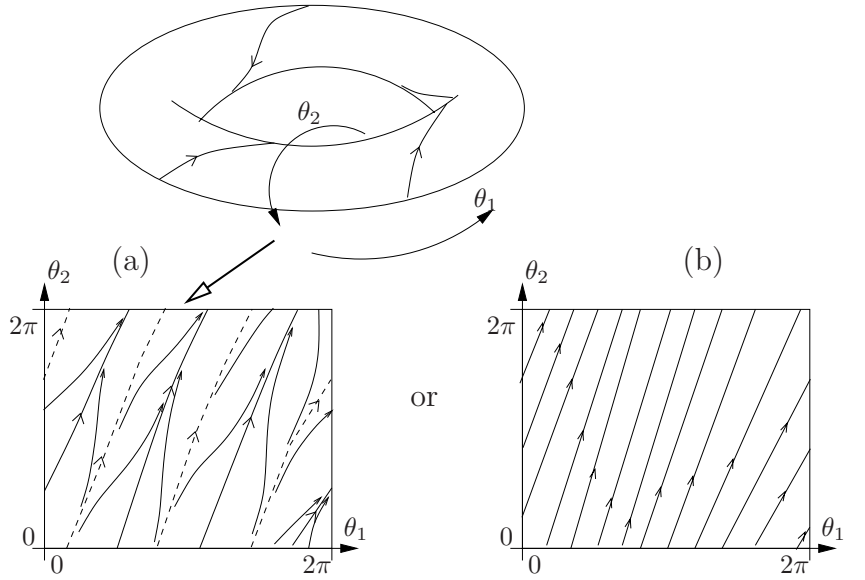

Fig. 2.3. Possible motion on an invariant torus, (a) phase locked, and (b) quasi-periodic.

Homoclinic and heteroclinic orbits. Another important class of invariant sets are *connecting orbits*, which tend to other invariant sets as time asymptotes to $+\infty$ and to $-\infty$. Consider, for example, orbits that connect equilibria. A *homoclinic orbit* is a trajectory $x(t)$ that connects an equilibrium x^* to itself; $x(t) \to x^*$ as $t \to \pm\infty$. A *heteroclinic orbit* connects two different equilibria x_1^* and x_2^*; $x(t) \to x_1^*$ as $t \to -\infty$ and $x(t) \to x_2^*$ as $t \to +\infty$. Homoclinic and heteroclinic orbits play an important role in separating the basins of attraction of other invariant sets.

Other invariant sets. It is quite possible for dynamical systems to contain certain simple geometric subsets of phase space where trajectories must remain for all time once they enter. For example, an ODE system written in the form

$$\begin{aligned}\dot{x}_1 &= f_1(x_1, x_2, x_3)\\ \dot{x}_2 &= x_1 f_2(x_1, x_2, x_3)\\ \dot{x}_3 &= x_1 f_3(x_1, x_2, x_3)\end{aligned}$$

for smooth functions f_i, $i = 1, \ldots, 3$ has as an invariant set the plane $\{(x_1, x_2, x_3) \in \mathbb{R}^3 : x_1 = 0\}$. The dynamics on this invariant plane could contain equilibria, periodic orbits and other attractors. Similarly, in addition to invariant tori, flows can contain invariant spheres, cylinders, etc. invariant sets that are everywhere locally smoothly described by an m-dimensional set of co-ordinates are called *invariant manifolds*, important

examples of which are stable and unstable manifolds of saddle points, which we shall encounter shortly.

Chaos. More complex invariant sets are *chaotic*, a term that might be defined in a number of different ways, but we suppose:

Definition 2.6. *A closed and bounded invariant set Λ is called* **chaotic** *if it satisfies the two additional conditions:*

1. *It has* **sensitive dependence on initial conditions***; i.e.:*

   There exists an $\varepsilon > 0$ such that, for any $x \in \Lambda$, and any neighborhood $U \subset \Lambda$ of x, there exists $y \in U$ and $t > 0$ such that $|\phi^t(x) - \phi^t(y)| > \varepsilon$
2. *There exists a* **dense trajectory** *that eventually visits arbitrarily close to every point of the attractor, i.e.:*

   There exists an $x \in \Omega$ such that for each point $y \in \Omega$ and each $\varepsilon > 0$ there exists a time t (which may be positive or negative) such that $|\phi^t(x) - y| < \varepsilon$.

The first property says that initial conditions in the invariant set diverge from each other locally. The second property says that there is at least one trajectory in the invariant set such that not only eventually comes back arbitrarily close to itself, but to *every* point of the invariant set. This property ensures that we are talking about an attractor composed of a single piece, not two separate ones. This property is also known as *topological transitivity*.

We saw several examples of chaotic attractors of non-smooth systems in Chapter 1. For flows (smooth or non-smooth), it can be shown that the dimension of phase space must be at least three in order for a flow to exhibit chaos. Various techniques for analyzing and quantifying chaotic motion exist, such as Lyapunov exponents, time series analysis, invariant measures, fractal dimension, etc. For a more thorough treatment of the statistical properties of chaos see for example the book by Sprott [242]. Some of these notions have counterparts in non-smooth systems, see for example the work of Kunze [165].

Flows naturally lead to maps through the process of taking a (Poincaré) section through the flow and considering the map of that section to itself induced by the flow; see Fig. 2.5. We will make this important concept precise in Sec. 2.1.5 below.

2.1.2 Iterated maps

Given a **map** defined by the rule

$$x \mapsto f(x), \quad x \in \mathcal{D} \subset \mathbb{R}^n, \tag{2.6}$$

then $T = \mathbb{Z}$; that is, 'time' is integer-valued, and the operator ϕ is just f. Evolving through time $m > 0$ involves taking the mth iterate of the map;

$$\phi^m(x_0) = x_m = f(x_{m-1}) = f(f(x_{m-2})) = \ldots := f^{(m)}(x_0),$$

where a superscript (m) means m-fold composition

$$f^{(m)}(x_0) = \overbrace{f \circ f \circ \ldots \circ f(x_0)}^{m \text{ times}}.$$

Again we shall write $f(x, \mu)$ for systems that depend on parameters $\mu \in \mathbb{R}^p$.

A useful way of studying one-dimensional maps is via *cobweb diagrams* that plot x_{n+1} against x_n by reflecting in the main diagonal

Example 2.2 (logistic map). An example of a cobweb diagram for the *logistic map* given by

$$x \to \mu x(1-x), \quad x \in [0,1], \quad 0 < \mu \leq 4 \tag{2.7}$$

is given in Fig. 2.4.

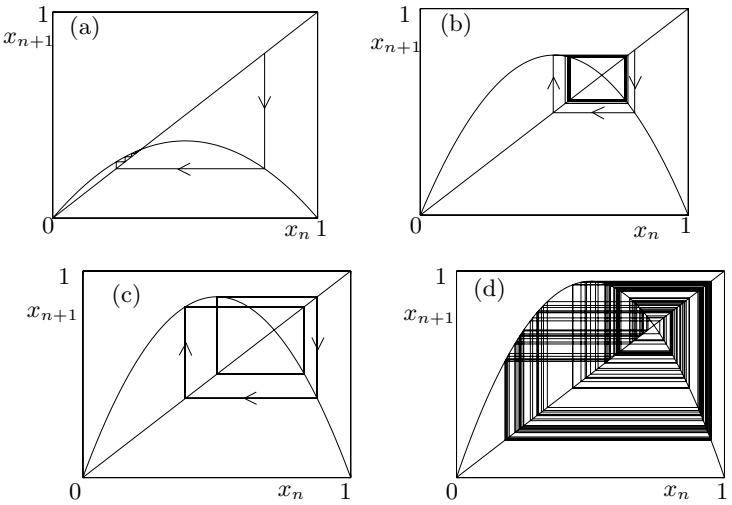

Fig. 2.4. Cobweb diagrams for the logistic map (2.7) starting with $x_0 = 0.8$ showing: (a) convergence to a stable fixed point for $\mu = 1.5$; (b) convergence to a period-two attractor for $\mu = 3.1$; (c) period-four attractor (note that here the initial condition is set to $x = 0.5$), and (d) chaotic behavior for $\mu = 4$.

Definition 2.7. *A mapping (2.6) is said to be* **invertible** *for $x \in \mathcal{D} \subset \mathbb{R}^n$ if given any $x_1 \in \mathcal{D}$ there is a* unique *$x_0 \in \mathcal{D}$ such that $x_1 = f(x_0)$. In such a case we define the inverse mapping $f^{(-1)}$ by $x_0 = f^{(-1)}(x_1)$ for all points x_1 in $f(\mathcal{D})$.*

Note that the smoothness of the dynamical system in the case of maps is given simply by the smoothness of the function f. Smooth (that is, at least

C^1) invertible maps, with smooth inverses are referred to as *diffeomorphisms*. We will now list some important types of invariant sets of maps.

fixed points. The simplest kind of invariant set of a map is a *fixed point*, which is a point x^* such that $f(x^*) = x^*$. fixed points of maps have a close connection to periodic orbits of flows, through the induced (Poincaré) map; see Fig. 2.5

periodic points. Next in order of complexity come periodic points, which satisfy $f^{(m)}(x^*) = x^*$ for some (least value of) $m > 0$. We refer to such a point as a *period-m point* of the map and its orbit as a period-m orbit. Clearly each point $f^{(i)}(x^*)$, $i \leq m-1$ of a period-m orbit is also a period-m point. These again are the close analogs of periodic orbits of flows (of a higher period), implying more intersections with a Poincaré section; see Fig. 2.5(b).

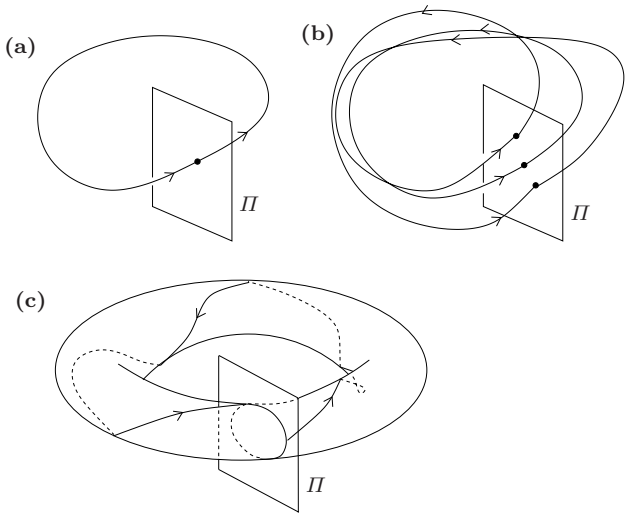

Fig. 2.5. Depicting the relation between maps and flows obtained by taking a Poincaré section Π through the phase space of the flow and considering the induced map from $\Pi \to \Pi$. (a) The correspondence between fixed points and period-T limit cycles; (b) between period-m points and higher-period limit cycles ($m = 3$ in this case); and (c) between invariant circles and invariant tori.

Invariant circles. Analogous to invariant tori of flows are *invariant closed curves* of a map, which again may be defined by taking a Poincaré section of a torus; see Fig. 2.5(c). Such closed curves are topologically circles, and we can reduce the dynamics *on* an invariant closed curve to that of a map of the unit circle to itself, a so-called *circle map*. The dynamics *off* or transverse to an invariant closed curve can also be complex. Typically, as

parameters vary, such curves lose their smoothness and eventually fail to exist as continuous invariant sets; see for example [9, 168, 8] for the kind of dynamics one expects under such bifurcation sequences for smooth systems. Recently Zhusubaliyev & Mosekilde [281, 282, 280] and Dankowicz, Piiroinen & Nordmark [65] found yet more complex bifurcation sequences can occur near an invariant circle of certain piecewise-smooth systems; we shall return to non-smooth circle maps in Chapter 4 and non-smooth torus bifurcations in Chapter 9.4.3. For comparison with the non-smooth case, we will recall here just a few standard results for the dynamics *on* smooth invariant circles. For more details, see for example the book by Arrowsmith and Place [9].
Consider a map $f : S^{(1)} \to S^{(1)}$, where $S^{(1)}$ is the unit circle.

Example 2.3 (Arnol'd circle map). A canonical example of a circle map is the Arnol'd circle map (or standard map)

$$\theta \to f(\theta) = \theta + \alpha + \varepsilon \sin(\theta) \pmod{2\pi}, \tag{2.8}$$

where $0 \leq \varepsilon < 1$. When $\varepsilon = 0$, clearly the map describes a rigid rotation through an angle α. If $\alpha = p/q$ is rational, then all points are periodic with period q. If α is irrational, then motion never repeats and all initial conditions θ_0 are quasi-periodic and $\cup_{n=1}^{\infty} f^{(n)}(\theta_0)$ fills out the entire circle. However, the dynamics is not chaotic since nearby initial conditions remain close.

For $\varepsilon > 0$, then one can use the notion of *rotation number* to define the equivalent of these two behaviors.

Definition 2.8. *Consider a circle map $f : S^{(1)} \to S^{(1)}$, which can be written in functional form as $\overline{f}(\theta \bmod 2\pi) \bmod 2\pi$, where $\overline{f} : \mathbb{R} \to \mathbb{R}$ is called a* lift *of f. We define the* **rotation number** *ρ of a point $x \in [0, 2\pi)$ by*

$$\rho(f, x) = \left(\lim_{n \to \infty} \frac{f^{(n)}(x) - x}{n} \right) \pmod{2\pi}. \tag{2.9}$$

Now, we have the standard result; see for example [73, 151]:

Theorem 2.1. *Suppose a circle map f is continuous and has a continuous inverse; then the rotation number is independent of initial condition x; that is, $\rho(f, x) = \rho(f)$.*

If the rotation number is irrational, it can be shown that (under the additional assumption that both the map f and its inverse are differentiable) the dynamics is topological equivalent to a rigid rotation through angle ρ; thus, the dynamics is non-chaotic and the forward iterate of any initial condition eventually fills the whole circle. In contrast, if $\rho = p/q$ is rational, then the dynamics is said to be *mode locked* and there is at least one orbit of period q. Typically there will be two such orbits, with one stable

and one unstable. Given a family of circle maps parameterized by α, then the rotation number will generically be rational over intervals of α-values. Both irrational and rational rotation numbers occur for sets of α-values that have positive measure. We will return to the study of circle maps in Chapter 4, where we show that they are closely linked to maps that are discontinuous on an interval.

Chaos. Definition 2.6 of chaotic invariant sets also applies to maps. In contrast to flows where the phase space must be at least three-dimensional, in the noninvertible case, maps of dimension one can exhibit chaos. We have already seen this for the square-root map in case study VII in Chapter 1. Smooth one-dimensional maps can be chaotic too, as the following well-known example shows:

Example 2.4 (logistic map continued). Consider again the logistic map (2.7). For $\mu > 1$, there are two fixed points at $x = 0$ and $x = (\mu - 1)/\mu$. For $1 < \mu < 3$, the non-trivial one is the unique attractor of the system. For $\mu > 3$, there are also two period-two points

$$x = \frac{1 + \mu \pm \sqrt{\mu^2 - 2\mu - 3}}{2\mu}.$$

As μ is further increased, a chaotic attractor is born via a so-called *period-doubling* cascade; see Fig. 2.6. Note that in the 'chaotic' range of μ-values, the attractor actually alternates between parameter intervals of chaos and intervals of periodic orbits (so-called *periodic windows*) appearing in the bifurcation diagram.

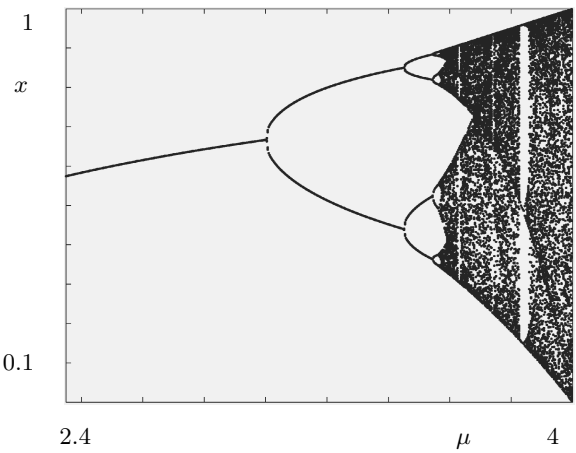

Fig. 2.6. The bifurcation diagram of the logistic map (2.7) showing the period-doubling cascade to chaos as the parameter μ is increased and the presence of periodic windows within the chaos.

For invertible maps, at least two dimensions are required in order for there to be chaotic invariant sets.

2.1.3 Asymptotic stability

When considering dynamical systems with physical application, we are usually only interested in stable behavior. Important notions of stability in dynamical systems include that of either *Lyapunov* or *asymptotic* stability of an invariant set. In general, the former means stability in the weak sense that trajectories starting nearby to the invariant set remain nearby for all time, whereas the latter is more or less synonymous with the concept of an attractor (Definition 2.3). Both refer to stability of invariant sets with respect to perturbations of initial conditions, at fixed parameter values. There are other less restrictive versions of this kind of stability, such as input–output stability, orbital stability, and controllability of arbitrary trajectories (not just invariant sets), but these will not concern us. For simplicity we shall define stability only of equilibria of flows. Similar definitions can be given for fixed points of discrete-time systems, or for other invariant sets of either continuous-time or discrete-time systems.

To formally define Lyapunov stability, consider a generic nonlinear system of the form (2.3) and assume that it has an equilibrium point that, without loss of generality, is at the origin; that is, $f(0) = 0$:

Definition 2.9. *The equilibrium state at the origin is said to be* **(Lyapunov) stable** *if for any $\varepsilon > 0$, there exists a $\delta > 0$ such that*

$$\|x_0\| < \delta \Rightarrow \|\Phi(x_0, t)\| < \varepsilon, \forall t > 0.$$

Definition 2.10. *The equilibrium state at the origin is said to be* **asymptotically stable** *(in the sense of Lyapunov) if*

1. *it is stable;*
2. $\lim_{t\to\infty}\Phi(x_0, t) = 0$.

We will say that an equilibrium is *unstable* if it is not stable according to Definition 2.9.

Thus, stability refers to the ultimate state of the dynamics not being altered under small changes to the initial conditions. For equilibria, the notion of stability is closely linked to the eigenvalues of the corresponding linearized ODEs, with a sufficient condition for stability being that all eigenvalues lie in the left half of the complex plane. Similar sufficient conditions for asymptotic stability exist for other invariant sets. For example, for fixed points of maps, stability is guaranteed if all eigenvalues (often called multipliers) of the linearization of the map lie inside the unit circle. Proving stability can be more tricky in the case that eigenvalues lie on the imaginary axis. One technique is to construct so-called *Lyapunov functions* that act like the energy of a perturbation from the invariant set in question, and then prove that this energy

decreases with time as one follows the dynamics. As we shall see in Sec. 2.4, for non-smooth systems, proving asymptotic stability even in the case of equilibria whose eigenvalues in the left half-plane can be highly tricky. There, the Lyapunov function technique can be extremely useful.

We next deal with a quite different notion of stability, that of invariance of the dynamics under perturbation to the system itself rather than to initial conditions.

2.1.4 Structural stability

Dynamical systems theory aims to classify dynamics qualitatively. structurally stable systems are ones for which all 'nearby' systems have qualitatively 'equivalent' dynamics. Thus we need a precise notion of *nearby* and also of *equivalence*.

'Nearby' refers to any possible perturbation of the system itself [the function $f(x)$], including variation of the system's parameters. We want to call two systems 'equivalent' if their phase spaces have the same dimension and there phase potraits contain the same number and type of invariant sets, which in the same general position with respect to each other. To achieve such a definition, we use topology, which is the mathematics of 'rubber sheet geometry.' Mathematically we want to say that two phase potraits are the same if there is a smooth transformation that stretches, squashes, rotates, but not folds one phase potrait into the other. Such transformations are called *homeomorphisms*, which are continuous functions defined over the entire phase space whose inverses are also continuous.

Definition 2.11. *Two dynamical systems* $\{X, T, \phi^t\}$ *and* $\{X, T, \psi^t\}$ *are* **topological equivalent** *if there is a homeomorphism* h *that maps the orbits of the first system onto orbits of the second one, preserving the direction of time.*

For discrete time systems, two topological equivalent maps f and g that satisfy

$$f(x) = h^{-1}(g(h(x))), \quad \text{implying} \quad h(f(x)) = g(h(x)),$$

for some homeomorphism h, are said to be topologically *conjugate*, and we can write more simply

$$f = h^{-1} \circ g \circ h. \tag{2.10}$$

For ODEs, the homeomorphism should apply at the level of the flow.

Definition 2.12. *Two flows* $\Phi(x,t)$ *and* $\Psi(h(x),t))$ *that correspond, respectively, to ODEs* $\dot{x} = f(x)$ *and* $\dot{y} = g(y)$ *are said to be* **topologically conjugate** *if there exists a homeomorphism* h *such that*

$$\Phi(x,t) = h^{-1}(\Psi(h(x),t)). \tag{2.11}$$

Actually, for topological equivalence of flows, the conjugacy does not need to apply at each time t. Rather, we require the weaker condition that there is an invertible, continuous mapping of time $t \mapsto s(t)$ so that we can write

$$\Phi(x,t) = h^{-1}(\Psi(h(x), s(t))) \,. \tag{2.12}$$

Note, though, that conditions (2.11) and (2.12) are hard to check in practice, because one must solve the ODE exactly in order to construct an explicit expression for the flow operator Φ. A more restrictive condition, which is easier to check in practice, is that two ODEs be *smoothly topologically conjugate*; that is, the homeomorphism h in (2.11) is differentiable, with differentiable inverse (a *diffeomorphism*). Then we can write

$$f(x) = \left(\frac{dh(x)}{dx}\right)^{-1} f(h(x)).$$

Having defined what we mean by topological equivalence, we can now define structural stability.

Definition 2.13. *A flow (or discrete-time map) is* **structurally stable** *if there is an $\varepsilon > 0$ such that all C^1 perturbations of maximum size ε to the vector field (map) f lead to topological equivalent phase potraits.*

One key application of topological equivalence is to show that 'normally' dynamical systems in the neighborhood of an invariant set are topological equivalent to the linearization of the system about that set. We consider this in the two specific contexts of equilibria of flows and fixed points of maps. As we shall see in the next subsection, the result for maps implies an analogous result for periodic orbits of flows.

Consider first an equilibrium x^* of $\dot{x} = f(x)$. Now, for small $y = x - x^*$, we can expand f as a Taylor series about x^* to write

$$\dot{y} = f_x(x^*)y + O(y^2),$$

and drop the $O(y^2)$-term. (Here $f_x(x^*)$ given by $(f_x)_{i,j} = \partial f_i/\partial x_j$ is the Jacobian derivative of the vector field evaluated at x^*.) The general solution to the linear system is

$$y(t) = \exp(f_x(x^*)t)y(0).$$

Usually this can be expressed in terms of the eigenvalues and eigenvectors of $f_x(x^*)$. For example, in the case that Jacobian has a full set of n independent eigenvalues $\{\lambda_i : i = 1, 2, \ldots n\}$, then we can write

$$y(t) = V^{-1}\mathrm{diag}\{e^{-\lambda_1 t}, e^{-\lambda_2 t}, \ldots e^{-\lambda_n t}\}Vy(0),$$

where the ith column of V contains the eigenvectors of f_x corresponding to eigenvalue λ_i. (Here diag$\{\cdot\}$ means the diagonal matrix whose entries on the main diagonal are those stated.) So if the spectrum (set of eigenvalues) of $f_x(x^*)$ is in the left half-plane, then the solution of the linear system tends to zero as $t \to \infty$ and the equilibrium of the linear system is stable.

Definition 2.14. *We shall refer to the* **eigenvalues** *of an equilibrium x^* of an ODE $\dot{x} = f(x)$ to mean the eigenvalues of the associated Jacobian matrix $f_x(x^*)$. An equilibrium is said to be* **hyperbolic** *if none of its eigenvalues lie on the imaginary axis.*

It can be proved [168, Ch. 2] that the flow local to any two hyperbolic equilibria of n-dimensional systems that have the same number of eigenvalues with negative real part are topologically equivalent to each other. In particular, we have

Theorem 2.2 (Hartman–Grobman). *The dynamics close to a hyperbolic equilibrium point are topologically equivalent to that of the system linearized about that point.*

An equilibrium x^* with $n_s > 0$ eigenvalues of negative real part and $n_u > 0$ eigenvalues of positive real part is called a saddle point. Close to x^* we can define the stable [unstable] manifold $W^s(x^*)$ [$W^u(x^*)$], which is an invariant manifold of the flow that is composed of all trajectories that tend to x^* as $t \to \infty$ ($t \to -\infty$). $W^s(x^*)$ is of dimension n_s and is tangent at x^* to the stable eigenspace of $f_x(x^*)$; similarly $W^s(x^*)$ is of dimension n_u and is tangent at x^* to the unstable eigenspace of $f_x(x^*)$. See Fig. 2.7.

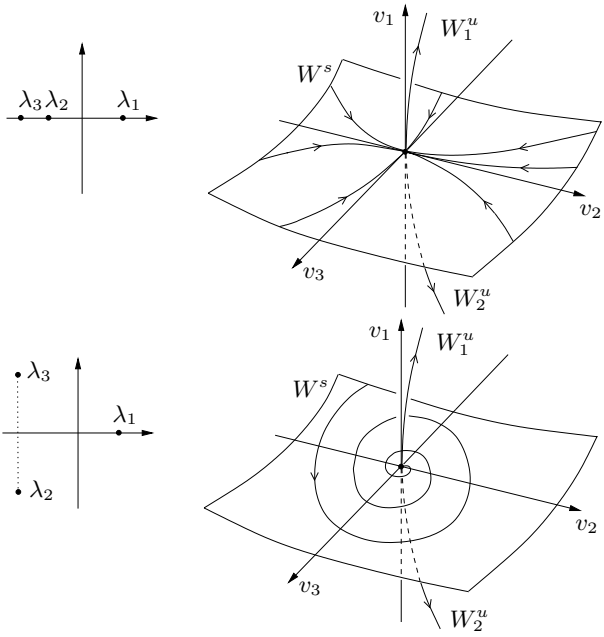

Fig. 2.7. Stable and unstable manifolds near 3 dimensional saddle equilibria with (a) purely real eigenvalues and (b) complex stable eigenvalues (*a saddle focus*). The vectors v_k are the eigenvectors corresponding to the eigenvalues λ_k.

Similarly, consider a fixed point x^* of a map $x \mapsto f(x)$ (period-m points can be treated as well, since they are fixed points of $f^{(m)}$). Linearizing about this fixed point, we get

$$y \mapsto f_x(x^*)y, \quad \text{with solution} \quad y_n = [f_x(x^*)]^n y_0.$$

Hence $y_i \to 0$ as $i \to \infty$, satisfying the second of the conditions for asymptotic stability of the linearized system, if all eigenvalues μ_i of $f_x(x^*)$ lie inside the unit circle.

Definition 2.15. *We shall refer to the* **multipliers** λ_i *of a fixed point* x^* *of a map* $x \to f(x)$ *to mean the eigenvalues of the associated linearization* $f_x(x^*)$. *A fixed point is said to be* **hyperbolic** *if none of the multipliers lie on the unit circle.*

For a general map in n-dimensions, one can define the *orientability* of the map close to a fixed point as the sign of the product of all its multipliers $\prod_{i=1}^{n} \lambda_i$. If this product is positive, the map is locally orientable; if negative, the map is non-orientable. If the product is zero, then the map is noninvertible. Note that any map that arises as the Poincaré mapof a smooth flow must be orientable [271]. Figure 2.8 shows the two possible types of orientable saddle point in two-dimensional maps. That with negative multipliers [Fig. 2.8(b)] is sometimes referred to as a *flip saddle*. One can also define stable and unstable

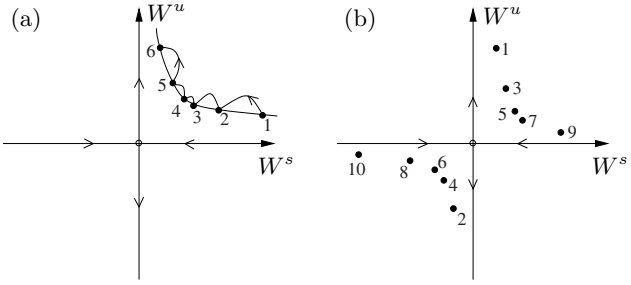

Fig. 2.8. The dynamics near a saddle fixed point of a map in the cases of (a) two positive multipliers, and (b) two negative multipliers. Numbers denote subsequent iterations of the map starting from the point labeled '1'.

manifolds at saddle points analogously as for equilibria of flows. Note, though, a distinction with the case of flows. In a flow, a one-dimensional manifold is composed of a single trajectory. In a map, a one-dimensional manifold contains many orbits; see Fig. 2.9. Hence stable and unstable manifolds in maps can intersect transversally (at a non-zero angle), whereas if a stable and unstable manifold intersect in a flow, they must do so along a line; that is, they must share a common trajectory.

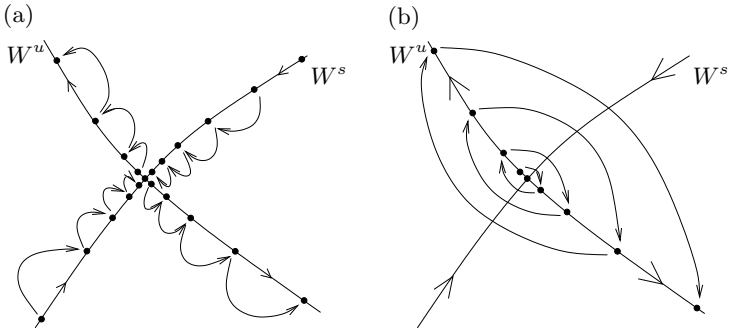

Fig. 2.9. (a) The stable and unstable manifolds close to a saddle fixed point in two dimensions with positive multipliers. (b) Similar figure in the case of negative multipliers, where, for clarity, only the dynamics along the unstable manifold is depicted. Similar behavior is observed on the stable manifold with the difference that the direction of 'hoppings' is reversed.

There are similar notions of hyperbolicity for other invariant sets. Loosely speaking, an invariant set is hyperbolic (sometimes called *normally hyperbolic*) if the dynamics in directions transverse to the set is exponentially attracting or repelling at rates that are faster than the dynamics in the invariant set. See, for example, [272]. Generally speaking, hyperbolic dynamics are structurally stable.

Many dynamical systems that arise in applications are not structurally stable. For example, systems can have persistent non-hyperbolic equilibria (center points) if they preserve a first integral such as energy. An important such class is that of Hamiltonian systems, which have very different dynamics than the systems in question here; see, for example, the reprint collection by Miess and MacKay [184]. Alternatively, the system may be invariant under the action of a symmetry, which again leads to certain structurally unstable things happening generically. The dynamics of systems with symmetry is a large subject in its own right, and one that we do not deal with here; see, for example, the book by Golubitsky, Schaeffer & Stewart [120]. Largely speaking, we shall avoid Hamiltonian or symmetric systems in what follows.

2.1.5 Periodic orbits and Poincaré maps

We have already hinted at the important connection between flows and maps. We now make this connection more precise. One of the main building blocks of the dynamics of a set of ODEs are its periodic solutions, and these provide a natural way to transform between flows and maps. Consider a limit cycle solution $x(t) = p(t)$ to (2.3) of period $T > 0$; that is, $p(t+T) = p(t)$. To study the dynamics near a such a cycle, we construct a *Poincaré section*, which is an $(n-1)$-dimensional surface Π that contains a point $x_p = p(t^*)$ on the limit cycle and which is *transverse* to the flow at x_p. Let us introduce a notation

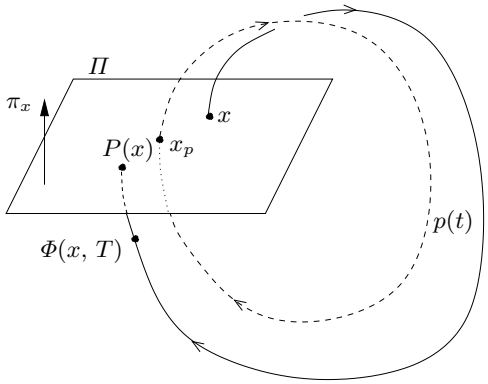

Fig. 2.10. The construction of a Poincaré mapclose to a periodic orbit $p(t)$.

that

$$\Pi = \{x \in \mathbb{R}^n : \pi(x) = 0\}, \tag{2.13}$$

for some smooth scalar function π. Then the transversality condition is that the normal vector $\pi_x(x_p)$ to Π at x_p has a non-zero component in the direction of the $\Phi_t(x_p, 0) = f(x_p)$. (Here a subscript x or t means differentiation with respect to that variable). That is, we require

$$\pi_x(x_p) f(x_p) \neq 0. \tag{2.14}$$

where a subscript x or t means partial differentiation with respect to that variable, so that $\pi_x(x_p)$ is the normal vector to Π at $x = x_p$.

Now, we can use the flow Φ to define a map P from Π to Π, called the *Poincaré map*, which is defined for x sufficiently close to x_p via

$$P(x) = \Phi(x, \tau(x)),$$

where $\tau(x)$ is defined implicitly as the time closest to T for which

$$\pi(\Phi(x, \tau(x))) = 0. \tag{2.15}$$

By the Implicit Function Theorem (see Theorem 2.4 below), the transversality (2.14) guarantees that there is a locally unique solution for $\tau(x)$. Note that we can then define the Poincaré mapas a *smooth projection* S of the time-T map $\Phi(\cdot, T)$ for $x \in \Pi$

$$P(x) = S(\Phi(x, T), x), \quad \text{where} \quad S(y, x) = \Phi(y, \tau(x) - T); \tag{2.16}$$

see Fig. 2.11. Thus, x_p becomes a fixed point of the map P.

We can study the stability (and possible bifurcations of) the periodic solution by studying the linearization P_x of the Poincaré map at x_p. It will be important for us to be able to compute this linearization when we consider

grazing bifurcations of periodic orbits in Chapters 6–8. Computing the total derivative with respect to x, we have

$$P_x(x_p) = \Phi_x(x_p, T) + \Phi_t(x_p, T)\tau_x(x_p),$$

and, from implicit differentiation of (2.15),

$$\tau_x(x_p) = -\frac{\pi_x(x_p)\Phi_x(x_p, T)}{\pi_x(x_p)\Phi_t(x_p, T)}.$$

Hence

$$\begin{aligned} P_x(x_p) &= \left(I - \frac{\Phi_t(x_p, T)\pi_x(x_p)}{\pi_x(x_p)\Phi_t(x_p, T)}\right)\Phi_x(x_p, T) \\ &= \left(I - \frac{f(x_p)\pi_x(x_p)}{\pi_x(x_p)f(x_p)}\right)\Phi_x(x_p, T). \end{aligned} \tag{2.17}$$

Note that (2.17) is a *rank-one update* of the time-T map $\Phi_x(x_p, T)$ around $p(t)$ (the multiplying factor is the linearization of S defined in (2.16)). The $n \times n$ matrix $\Phi_x(x_p, T)$ is referred to as the *Monodromy matrix* and corresponds to the fundamental solution matrix up to time T of the linear variational equations

$$\dot{y} = f_x(p(t))y, \tag{2.18}$$

around the periodic orbit $p(t)$. The direction of the flow $\Phi_t(x_p, t) = f(x_p)$ can easily be shown to solve (2.18) and, hence, $f(x_p)$ is an eigenvector of $\Phi_x(x_p, T)$ corresponding to the multiplier 1. Letting the expression (2.17) act on $f(x_p)$, we see that this corresponds to an eigenvalue 1 of the linearized Poincaré mapP_x. However, since this eigenvector does not lie in the linear approximation to Π we will never see its effect when computing the Poincaré maptaking only points $x \in \Pi$.

Other than this trivial eigenvalue, the eigenvalues of the Monodromy matrix are precisely the multipliers λ_i of the Poincaré map. This can be argued as follows (see for example [168, Thm. 1.6] for a more careful proof). The nontrivial eigenvectors of the Monodromy matrix form an $(n-1)$-dimensional invariant subspace $\tilde{\Pi}$, say, that does not contain the direction $f(x_p)$. Hence $\tilde{\Pi}$ can be chosen to be a Poincaré section, as it satisfies the transversality condition (2.14). Now all we need to show is that the multipliers of two Poincaré maps P and $\tilde{P}$ defined via two different sections Π and $\tilde{\Pi}$ are the same. Let Π be given by (2.13), (2.15), and let $\tilde{\Pi} := \{x : \tilde{\pi}(x, \tilde{\tau}(x)) = 0\}$. The equivalence of these two maps arises because we can write

$$\tilde{P} = \tilde{S}^{-1} \circ P \circ \tilde{S}, \quad \text{where} \quad \tilde{S}(x) = \Phi(x, \tau(x) - \tilde{\tau}(x)), \tag{2.19}$$

where $\tilde{S}$ is the smooth mapping that takes points in $\tilde{\Pi}$ to Π using the flow; see Fig. 2.11(b). Linearizing (2.19) we obtain that

$$\tilde{P}_x = \tilde{S}_x^{-1} P_x \tilde{S}_x.$$

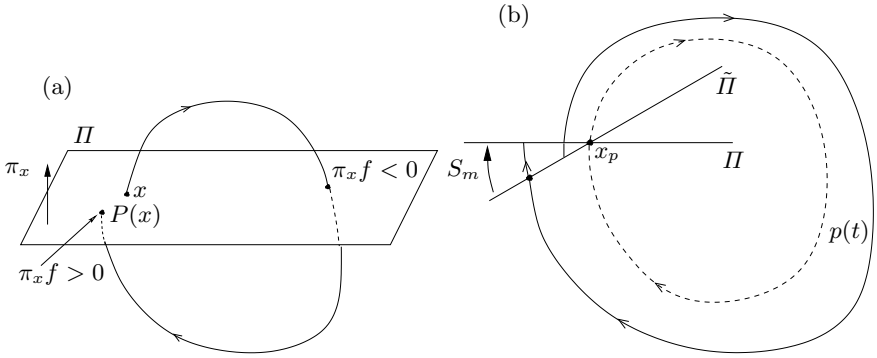

Fig. 2.11. (a) Illustrating a Poincaré mapdefined by the first intersection with a surface $\Pi : \{\pi(x) = 0\}$ in the direction of increasing $\pi(x)$. (b) A representation in two dimensions of the smooth projection S_m along the flow lines between Poincaré sections Π and $\tilde{\Pi}$.

Hence $\tilde{P}_x$ and P_x are *similar* matrices that must have the same eigenvalues. In fact, the expression (2.19) applies for any two Poincaré sections along the orbit $p(t)$. It also shows that the two Poincaré maps satisfy the condition (2.10) to be topological equivalent. Summarizing, we have

Theorem 2.3. *All Poincaré maps defined with respect to any Poincaré section that is transverse to the flow around a periodic orbit $p(t)$ of a smooth ODE (2.3) are locally topological equivalent. Moreover, they have the same non-zero multipliers $\lambda_1, \ldots \lambda_{n-1}$. The linearization of the corresponding time-T map around $p(t)$ is related by the formula (2.17) and has eigenvalues $1, \lambda_1, \ldots \lambda_{n-1}$.*

Now, we say that a *hyperbolic* periodic orbit $p(t)$ is one whose Poincaré maphas multipliers λ_i, $i = 1, \ldots n-1$ that are all off the unit circle. The Hartman–Grobman theorem for maps then tells us that flow around the orbit is locally topologically equivalent to the linearization. An obvious consequence of this is that hyperbolic periodic orbits are necessarily isolated in phase space.

Poincaré maps do not necessarily require a periodic orbit in order to be defined. A Poincaré section Π can be taken anywhere in the phase space, provided the flow is everywhere transverse to it, as for example in Fig. 2.5(c) where Π is chosen transverse to the flow on an invariant torus. For transversality, we require that a condition equivalent to (2.14) applies throughout Π. So if we define Π as before to be the zero-set of a smooth function (2.13), then we are only interested in defining a Poincaré mapfor points x for which

$$\pi(x) = 0 \quad \text{and} \quad \pi_x(x)f(x) \neq 0.$$

The map is defined by the first intersection with Π *in the same sense*. That is, $P(x) = \Phi(x, \tau(x))$, where $\tau(x)$ is the first time $t > 0$ such that $\pi(\Phi(x,t)) = 0$ and $\pi_x f(\Phi(x,0)) \cdot \pi_x f(\Phi(x,t)) > 0$; see Fig. 2.11(a). Note that the map P

may not be defined for the whole Poincaré section, since not all points need to return.

One of the benefits of studying Poincaré maps rather than flows is that they drop by one the dimension of the sets we need to consider. Thus, limit cycles of flows correspond to isolated fixed points of Poincaré maps; invariant tori correspond to closed curves of the map; and chaotic invariant sets decrease their fractal dimension by one.

2.1.6 Bifurcations of smooth systems

Broadly speaking, there two notions of 'bifurcation', one analytical and the other topological. From the first point of view, bifurcations are branching points of parameterized sets of solutions $x(\mu)$ to nonlinear operators $G(x, \mu) = 0$. Simply put, a 'bifurcation' is a point at which the Implicit Function Theorem fails; see, for example, [141, 55, 47, 119]).

Theorem 2.4 (Implicit Function Theorem). *Suppose that for some $\mu = \mu_0$ there exists a solution $x = x_0$ to a smooth nonlinear equation $G(x, \mu) = 0$, where $G : \mathbb{R}^n \times \mathbb{R} \to \mathbb{R}^n$; then, provided $G_x(x_0, \mu_0)$ is nonsingular, a smooth path of solutions $x(\mu)$ can be continued locally, with $x(\mu_0) = x_0$.*

This analytic point of view does not adapt naturally to the study of non-smooth systems, and so the notion adopted in this book is that a bifurcation is a change in the topology of the phase portraits of a dynamical system as a parameter is varied. Of particular importance are changes to the number and nature of the attractors of the system. A rich theory now exists for smooth systems, which we shall briefly review here. Many more details can be found in the books by Guckenheimer & Holmes [124], Kuznetsov [168] and Wiggins [273]; hence, we give only a quick introduction to bifurcation theory applied to parameterized systems either in the form of a smooth vector field or map

$$\dot{x} = f(x, \mu), \quad \text{or} \quad x \mapsto f(x, \mu) \tag{2.20}$$

for $x \in \mathbb{R}^n$, $\mu \in \mathbb{R}^p$.

We define a bifurcation simply in terms of loss of structural stability upon varying a parameter.

Definition 2.16. *A* **bifurcation** *occurs at a parameter value μ_0 if the dynamical system $\{X, T, \phi^t\}$ is not structurally stable.*

An **unfolding** *(or* versal unfolding*) of a bifurcation is a simplified system that for small $\mu - \mu_0$ contains all possible structurally stable phase potraits that arise under small perturbations of the system at the bifurcation point.*

The **codimension** *of a bifurcation is the dimension of parameter space required to unfold the bifurcation.*

A **bifurcation diagram** *is a plot of (some measure of) the invariant sets of a dynamical system against a single bifurcation parameter μ, which indicates stability.*

We can distinguish between two kinds of bifurcation:

Definition 2.17. *A* **local bifurcation** *arises due to the loss of hyperbolicity of an invariant set upon varying a parameter. All other bifurcations are called* **global bifurcations**.

Many kinds of local bifurcations of smooth systems have been studied and classified; see for example Kuznetsov [165, Chs. 2–5]. Figure 2.12 summarizes the main types of codimension-one *local bifurcations* of smooth vector fields and an associated representative bifurcation diagram. In each case, under appropriate defining and non-degeneracy conditions, one can calculate an appropriate *normal form* that can be obtained by smooth co-ordinate transformations from any system that undergoes the bifurcation in question.

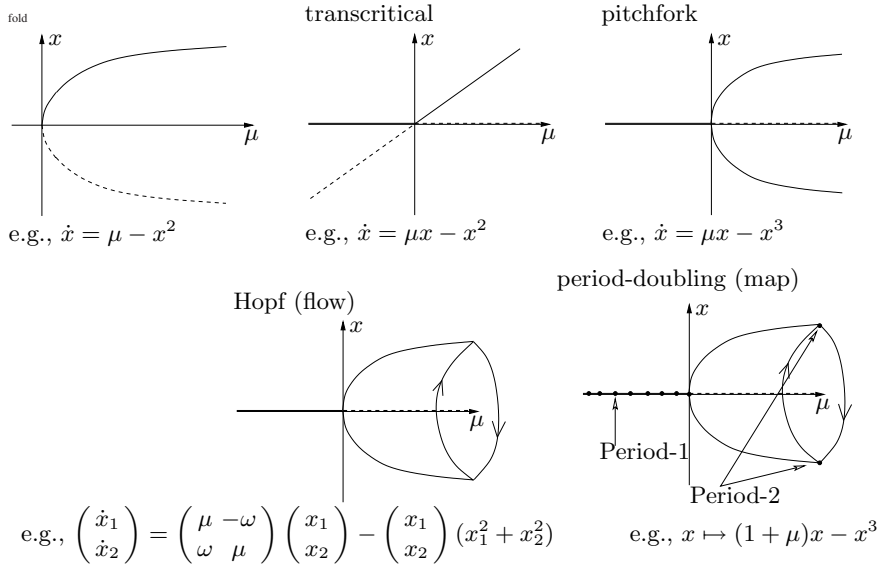

Fig. 2.12. Main codimension-one local bifurcations in smooth dynamical systems.

Note that steady bifurcations of equilibria of flows— fold (or saddle-node) bifurcations and the associated pitchfork or transcritical bifurcations for systems with symmetry or invariance— have a direct analogy for limit cycle bifurcations; that is, bifurcations of fixed points of maps. The defining condition for the former is that there is an eigenvalue at zero and for the latter that there is a multiplier at 1. The case of the Hopf bifurcation is more subtle. The direct analog for maps is when a complex pair of eigenvalues crosses the unit circle. This *torus* or *Neimark–Sacker* bifurcation causes the birth of invariant circles of the map, with all inherent complications associated with the dynamics of circle maps that we outlined earlier. There are also special cases when the multipliers concerned are low-order roots of unity. Finally, for

maps there is the case of the *period-doubling* or *flip* bifurcation, which has no analog in equilibrium bifurcations. Many of these bifurcations come in *super-* or *subcritical* subcases, depending on whether a stable nontrivial invariant set is created as the trivial equilibrium (or fixed point) becomes unstable, or vice versa.

In contrast, global bifurcations typically occur because of a change in the topology of stable and unstable manifolds of invariant sets (see, for example, [168, Chs. 6 and 7]). A typical example is a *homoclinic bifurcation* when the stable and unstable manifold of the same invariant set form an intersection or tangency at a fixed parameter value. See Fig. 2.13 for two examples. Also, stable and unstable manifolds of other invariant sets can form an intersection in a *heteroclinic connection* that can cause the sudden appearance or disappearance of a chaotic attractor in a *boundary crisis* bifurcation [168].

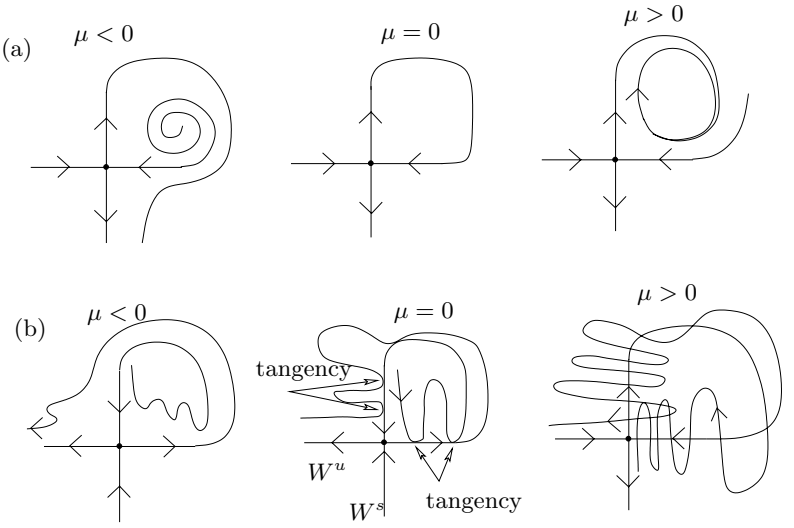

Fig. 2.13. Two global bifurcations. (a) A homoclinic bifurcation to a saddle equilibrium creating a single stable limit cycle. (b) A homoclinic tangency to a saddle point in a two-dimensional map creating a homoclinic tangle, which implies the existence of a chaotic invariant set through the Smale-Birkhoff homoclinic theorem [124, Thm. 5.3.5].

An interesting feature of smooth dynamical systems is that they can exhibit a *cascade* of local bifurcations under parameter variation. A well-known example is the period-doubling cascade. Here, a supercritical period-doubling at a parameter value μ_1 creates a stable period-2 orbit, followed by a further period-doubling of the period-2 orbit at $\mu = \mu_2$, creating a stable period-4 orbit, and so on, as we saw in Fig. 2.6. Remarkably, we observe a universal scaling law, established by Feigenbaum [97], that

$$\lim_{k\to\infty} \frac{\mu_k - \mu_{k-1}}{\mu_{k+1} - \mu_i} = \delta = 4.6692\ldots. \tag{2.21}$$

That is, the period-doubling sequence converges to a finite μ-value, and in the limit, the rate of convergence is the same for 'all' systems! For more precise details see, for example, [56, 73]. This universality of the period-doubling cascade has only been shown for a certain class of one-dimensional maps that have 'a single hump' like the logistic map, but it also applies to many ODEs because of the folded structure of their Poincaré maps. For one-dimensional maps, one can say much more, and we find cascades of periodic orbits described by the following theorem

Theorem 2.5 (Sharkovskii [235]). *Consider the following ordering of all positive integers:*

$$\begin{aligned}
&1 < 2 < 4 < \ldots 2^k < 2^k + 1 < \ldots \\
&\ldots \\
&< 2^{k+1}\cdot(2l+1) < 2^{k+1}\cdot(2l-1) < \ldots < 2^{k+1}\cdot 5 < 2^{k+1}\cdot 3 < \\
&\ldots < 2^k\cdot(2l+1) < 2^k\cdot(2l-1) < \ldots < 2^k\cdot 5 < 2^k\cdot 3 < \\
&\ldots \\
&\ldots < 2\cdot(2l+1) < 2\cdot(2l-1) < \ldots < 2\cdot 5 < 2\cdot 3 < \\
&\ldots < (2l+1) < (2l-1) < \ldots < 5 < 3.
\end{aligned}$$

If f is a continuous map of the interval $[-1,1]$ to itself with a periodic point of period p, then, for any $q < p$ (where the inequality sign refers to the ordering above), f has a periodic point of period q.

Remarks

1. This result contains the statement 'period 3 implies chaos' that was the title of the paper by Li & Yorke [178] from which the word *chaos* was first used to describe bounded non-repeating motion.
2. Often in applications a period-q ($q \neq 2^k$) orbit first appears by a fold bifurcation upon increasing a parameter beyond the end of a period-doubling cascade. This leads to a *periodic window* of parameter values within which this orbit is stable, with the windows separated by chaotic regions. Thus the Sharkovskii ordering often gives the ordering of stable periodic windows that are observed in simulations of bifurcation diagrams 'inside' the chaotic regime after the end of period-doubling cascade (see, for example, Fig. 2.6).

Sharkovskii's Theorem relies heavily on the smoothness assumption for the map. An important feature of this book, and especially the results in Chapters 3 and 4, will be the identification of other types of cascades of stable periodic orbits close to a bifurcation point. We shall see that these cascades do not generally follow the Sharkovskii ordering, in that either the chaos is *robust*

(i.e., has no periodic windows), or if windows exist they obey *period-adding* type orderings for which we see intervals of periodic motions of period n obeying the simple ordering $n < n+1 < n+2 < \ldots$. Indeed, as we shall see, period-adding is one of the unifying features of the behavior of non-smooth systems.

2.2 Piecewise-smooth dynamical systems

We now move onto the main theme of this chapter where we set the scene for a systematic study of the dynamics of non-smooth systems. Motivated by the case studies in Chapter 1, we shall introduce three classes of piecewise-smooth system: *maps*, *flows* and *hybrid systems*. Note that a complete existence and uniqueness theory does not exist, as far as we are aware, for these quite broad classes of system. Instead, in Sec. 2.3 below, we shall show the relation of these classes to other more precise formulations for the description of non-smooth dynamics for which such theory does exist. Nevertheless, our rather loose classification, while perhaps lacking mathematical rigor, shall prove highly useful in explaining the dynamics observed in example systems.

2.2.1 Piecewise-smooth maps

Definition 2.18. *A* **piecewise-smooth map** *is described by a finite set of smooth maps*

$$x \mapsto F_i(x, \mu), \quad \textit{for} \quad x \in S_i, \tag{2.22}$$

where $\cup_i S_i = \mathcal{D} \subset \mathbb{R}^n$ *and each* S_i *has a non-empty interior. The intersection* Σ_{ij} *between the closure (set plus its boundary) of the sets* S_i *and* S_j *(that is,* $\Sigma_{ij} := \bar{S}_i \cap \bar{S}_j$*) is either an* $\mathbb{R}^{(n-1)}$*-dimensional manifold included in the boundaries* ∂S_j *and* ∂S_i*, or is the empty set. Each function* F_i *is smooth in both the state* x *and the parameter* μ *for any open subset* U *of* S_i*.*

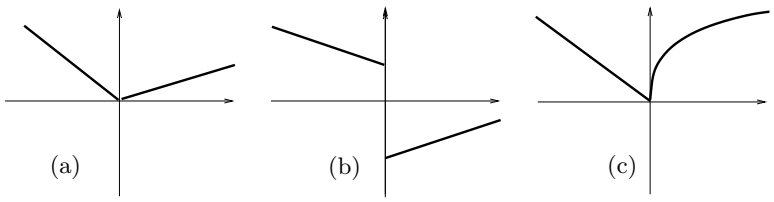

Fig. 2.14. Examples of piecewise-smooth one-dimensional maps: (a) piecewise-linear continuous map; (b) piecewise-linear discontinuous map; (c) square-root piecewise smooth map. In each case $S_1 = \{x < 0\}$, $S_2 = \{x > 0\}$ and $\Sigma_{12} = \{x = 0\}$.

A set Σ_{ij} for a piecewise-smooth map is usually termed a **border** or **discontinuity boundary** that separates regions of phase space where different smooth maps apply. Examples of piecewise-smooth one-dimensional maps are given in Fig. 2.14. Note that in the above definition we allow the possibility that one of the component maps F_i may itself be non-smooth (in the sense of having infinite or ill-defined derivatives) at the boundary Σ_{ij}. For example, the square-root map in Fig. 2.14(a) is such that the first derivative of $F_2(x)$ tends to ∞ as $x \to 0$. We also include the case that $F_i \neq F_j$ along Σ_{ij}, so that the map has a jump in state as in Fig. 2.14(b). Such maps are discontinuous piecewise-smooth maps. In this case, there are a number of choices that one can make about the value of the map for points in Σ_{ij}: for example, taking the average of F_i and F_j there; or allowing the map to be set valued at this point, taking all possible convex combinations $\{F_i + \lambda(F_j - F_i) : 0 \leq \lambda \leq 1\}$. In practice, such choices make little practical difference to the dynamics of the map, since they describe what happens to a set of points of zero measure.

Definition 2.19. *The* **order of singularity** *of a point $\widehat{x} \in \Sigma_{ij}$ of a continuous piecewise-smooth map is the order of the first non-zero term in the formal power-series expansion of $F_1(x) - F_2(x)$ about $x = \widehat{x}$.*

Remarks

1. This order is -1 times the usual definition of the order of a singularity in complex variable theory. That is, a complex $f(z)$ is said to have a pole with singularity of $O(n)$ if its Laurant series expansion starts with a term of order z^{-n}. Here we are saying that the map has singularity of order n if the Taylor series expansion of $F_1(x) - F_2(x)$ starts with a term of order x^n.
2. Note that we allow this order to be non-integer:

   Example 2.5 (square-root map). Consider the square-root map described in case study VII. According to the functional form (1.32), we have

   $$S_1 = \{x < \sigma\}, \quad S_2 = \{x > \sigma\}, \quad \Sigma_{12} = \{x = \sigma\},$$

   $$F_1 = \sqrt{\sigma - x} + r\sigma, \quad F_2 = rx,$$

   and hence

   $$[F_1 - F_2](\sigma + \varepsilon) = \varepsilon^{1/2} + O(\varepsilon).$$

   In this case we say that this map has an $O(1/2)$ singularity.

Maps that are locally piecewise-linear and continuous such as Fig. 2.14(a) and case study VIII are said to have an $O(1)$ singularity. Clearly differentiation of these one-dimensional maps with respect to x leads to maps with singularities of one order lower. For this reason we shall say that a point of discontinuity of a map with a jump, as in Fig. 2.14(b) and the heart attack map, case study VI, has an $O(0)$ singularity at a point $x \in \Sigma_{ij}$ if $0 < \|F_1(x) - F_2(x)\| < \infty$.

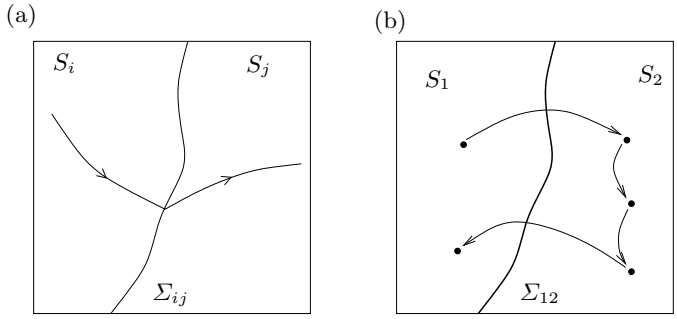

Fig. 2.15. Illustrating schematically trajectories of (a) a piecewise-smooth flow, and (b) a piecewise-smooth map.

2.2.2 Piecewise-smooth ODEs

Definition 2.20. *A* **piecewise-smooth flow** *is given by a finite set of ODEs*

$$\dot{x} = F_i(x, \mu), \quad \textit{for} \quad x \in S_i, \tag{2.23}$$

where $\cup_i S_i = \mathcal{D} \subset \mathbb{R}^n$ *and each* S_i *has a non-empty interior. The intersection* $\Sigma_{ij} := \bar{S}_i \cap \bar{S}_j$ *is either an* $\mathbb{R}^{(n-1)}$*-dimensional manifold included in the boundaries* ∂S_j *and* ∂S_i*, or is the empty set. Each vector field* F_i *is smooth in both the state* x *and the parameter* μ*, and defines a smooth flow* $\Phi_i(x,t)$ *within any open set* $U \supset S_i$*. In particular, each flow* Φ_i *is well defined on both sides of the boundary* ∂S_j*.*

A non-empty border between two regions Σ_{ij} will be called a **discontinuity set**, **discontinuity boundary** or, sometimes, a **switching manifold**. We suppose that each piece of Σ_{ij} is of codimension-one, i.e., is an $(n-1)$-dimensional smooth *manifold* (something locally diffeomorphic to $\mathbb{R}^n$) embedded within the n-dimensional phase space. Moreover, we shall demand that each such Σ_{ij} is itself piecewise-smooth. That is, it is composed of finitely many pieces that are as smooth as the flow. See Fig. 2.15(a).

Note that Definition 2.20 does not uniquely specify a rule for the evolution of the dynamics within a discontinuity set. One possibility is to assign each Σ_{ij} as belonging to a single region $\bar{S}_i$ only. That is, F_i rather than F_j applies on Σ_{ij}. In fact, such notions make little difference except in the case where the flow becomes confined to the boundary (Filippov trajectories). Before we get to that case, let us first consider what might happen to the flow of the piecewise-smooth ODE as we cross a discontinuity boundary Σ_{ij}.

Definition 2.21. *The* **degree of smoothness** *at a point* x_0 *in a switching set* Σ_{ij} *of a piecewise-smooth ODE is the highest order* r *such the Taylor series expansions of* $\Phi_i(x_0,t)$ *and* $\Phi_j(x_0,t)$ *with respect to* t*, evaluated at* $t=0$*, agree up to terms of* $O(t^{r-1})$*. That is, the first non-zero partial derivative with respect to* t *of the difference* $[\Phi_i(x_0,t) - \Phi_j(x_0,t)]|_{t=0}$ *is of order* r*.*

Remarks

- This definition almost accords with the usual definition of smooth functions, thinking of the flow at a point as being a function of t. Thus, if we say that a piecewise-smooth flow has degree of smoothness r across a discontinuity boundary, then it is C^{r-1} but not C^r. The vector field is one degree less smooth (because it is by definition the time derivative of the flow). Thus for a flow with degree of smoothness r according to the definition, the vector field will be C^{r-2} but not C^{r-1}.
- Note the subtle distinction between this definition and the corresponding Definition 2.19 for the singularity of a map. Here we do not allow the possibility for the degree of smoothness to be non-integer. [Although there is a growing literature on differential equations with fractional order right-hand sides (see, for example, [155]) we shall not treat them here.]

Now, consider an ODE local to a single discontinuity set Σ_{12} that can be written

$$\dot{x} = \begin{cases} F_1(x,\mu), & \text{if } x \in S_1 \\ F_2(x,\mu), & \text{if } x \in S_2 \end{cases},$$

where F_1 generates a flow Φ_1, F_2 a flow Φ_2. We have

$$\left.\frac{\partial \Phi_i(x,t)}{\partial t}\right|_{t=0} = F_i(x),$$

$$\left.\frac{\partial^2 \Phi_i(x,t)}{\partial t^2}\right|_{t=0} = \frac{\partial F_i}{\partial t} = \frac{\partial F_i}{\partial \Phi_i}\frac{\partial \Phi_i}{\partial t} = F_{i,x}F_i(x),$$

where a second subscript x means partial differentiation with respect to x. Similarly

$$\left.\frac{\partial^3 \Phi_i(x,t)}{\partial t^3}\right|_{t=0} = F_{i,xx}F_i^2 + F_{i,x}^2 F_i,$$

etc. So, if F_1 and F_2 differ in an mth partial derivative with respect to the state x, we find that the flows Φ_1 and Φ_2 differ in their $(m+1)$st partial derivative with respect to t.

Therefore, if $F_1(x) \neq F_2(x)$ at a point $x \in \Sigma_{12}$, then we have degree of smoothness one there. Systems with degree one are said to be of *Filippov* type. Examples of Filippov systems from Chapter 1 include case studies III, IV and V; the relay controller, friction oscillator and DC–DC converter examples.

Alternatively if $F_1(x) = F_2(x)$ but there is a difference in the Jacobian derivatives $F_{1,x} \neq F_{2,x}$ at x, then the degree of smoothness is said to be 2. A difference in the second-derivative tensor $F_{1,xx} \neq F_{2,xx}$ gives smoothness of degree three, etc. Systems with smoothness of degree two or higher may be called *piecewise-smooth continuous systems*, typified by the next example

Example 2.6 (bi-linear oscillator). The bi-linear oscillator, case study II, can be written as the first-order system by setting $u = x_1$,$v = x_2$ and $t = x_3$ so that

$$\dot{x}_1 = x_2 \tag{2.24}$$
$$\dot{x}_2 = -2\zeta x_2 - k_i x_1 + \cos(x_3) \tag{2.25}$$
$$\dot{x}_3 = 1. \tag{2.26}$$

where the value of k_i depends on region S_i, with $S_1 = \{x_1 < 0\}$, $S_2 = \{x_1 > 0\}$. Clearly the flow here has degree of smoothness two at all points in $\Sigma = \{x_1 = 0\}$. If instead $k_1 = k_2$ and the coefficient ζ in (2.24)–(2.26) had been allowed to vary across Σ, then the degree of smoothness would be one, at all points in Σ except where $x_2 = 0$; in which case, the degree would be two. Thus we have cases where the degree of smoothness is the same at all points in Σ and cases where it is not. This distinction shall become crucial when we consider grazing bifurcations in Chapters 6 and 7.

Definition 2.22. *A discontinuity boundary Σ_{ij} is said to be* **uniformly discontinuous** *in some domain $\mathcal{D}$ if the degree of smoothness of the system is the same for all points $x \in \Sigma_{ij} \cap \mathcal{D}$. We say that the discontinuity is* **uniform with degree m** *if the first non-zero partial derivative of $F_i - F_j$ evaluated on Σ_{ij} is of order $m-1$. Furthermore, the degree of smoothness is one if $F_i(x) - F_j(x) \neq 0$ for $x \in \Sigma_{ij} \cap \mathcal{D}$.*

In fact, the assumption of uniform discontinuity imposes a great restriction on the form that $F_i - F_j$ can take. Consider a general piecewise-smooth continuous system with a single boundary Σ that can be written as the zero set of a smooth function H

$$\dot{x} = \begin{cases} F_1(x), & H(x) > 0, \\ F_2(x), & H(x) < 0, \end{cases} \tag{2.27}$$

where $F_1(x) = F_2(x)$ if $H(x) = 0$. Suppose that the flow is uniformly discontinuous with degree m as in Definition 2.22. Then local to $H = 0$ we must be able to write

$$F_2(x) = F_1(x) + J(x)H(x)^{m-1}, \tag{2.28}$$

for some smooth function $J(x) \in \mathbb{R}^n$. To see this, note that H may locally be chosen as one of the co-ordinates close to the boundary and that a non-zero coefficient of $H(x)^k$ in the Taylor series expansion of $F_2 - F_1$, for $k < m-1$, means that the kth derivative of $F_2 - F_1$ does not vanish on Σ. Hence H^{m-1} must be a factor of $F_2 - F_1$. For example, for the bi-linear oscillator (2.24)–(2.26), which has $m = 2$, we have $H(x) = x_1$ and $J(x) = (0, -k_2 + k_1, 0)^T$.

2.2.3 Filippov systems

The case of systems a with uniform degree of smoothness one must be treated with great care since we have to allow the possibility of sliding motion. In order to define sliding, it is useful to think of a system (2.27) local to a discontinuity boundary between two regions defined by the zero set of a smooth function $H(x) = 0$; see Fig. 2.16.

Definition 2.23. *The* **sliding region** *of the discontinuity set of a system of the form (2.27) with uniform degree of smoothness one is given by that portion of the boundary of $H(x)$ for which*

$$(H_x F_1) \cdot (H_x F_2) < 0.$$

That is, $H_x F_1$ (the component of F_1 normal to H) has the opposite sign to $H_x F_2$. Thus, the boundary is simultaneously attracting (or repelling) from both sides.

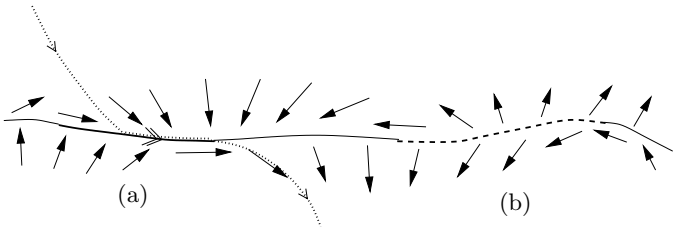

Fig. 2.16. A typical discontinuity boundary of a two-dimensional Filippov system showing the behavior of the vector fields on both sides. Bold and dashed regions represent (a) attracting and (b) repelling sliding motion, respectively. Dotted lines indicate three individual trajectory segments.

Note that the case of most interest is when the sliding region is attracting since, as is clear from Fig. 2.16, repelling sliding motion cannot be reached by following the system flow forward in time. However, attracting sliding motion can be reached in finite time. Henceforth, sliding will always be taken to mean 'attracting sliding' unless otherwise stated. Such motion leads to loss of information on initial conditions. Compare for example the two trajectories A and B of the two-dimensional flow represented in Fig: 2.16; they enter the sliding region at different points, but leave at the same point. Thus while they came from different initial conditions in the past, their future evolution is identical (the trajectory segment C). Thus, there is an infinite rate of attraction in forward time and the flow is not uniquely defined in reverse time. Another simple example of non-inevitability in mechanics is that of plastic impacts (e.g., imagine dropping a mature tomato on the floor!). Whatever the pre-impact velocity, the post-impact velocity is always zero.

As a consequence, any Poincaré mapassociated with trajectories that involve sliding motion will be noninvertible and have a multiplier that is zero (corresponding to the infinite rate of attraction). Now, the formalism of piecewise-smooth systems itself does not say how to define the evolution of the system as it undergoes sliding. One has to do something extra.

Two approaches exist in the literature for formulating the equations for flows that slide when written in the general form (2.27). These are *Utkin's*

equivalent control method [257] and *Filippov's convex method* [100]. In Utkin's method one supposes that the system flows according to the sliding vector field F_{12}, which is the average of the two vector fields F_1 (in region S_1) and F_2 (in region S_2) plus a control $\beta(x) \in [-1, 1]$ in the direction of the difference between the vector fields:

$$F_{12} = \frac{F_1 + F_2}{2} + \frac{F_2 - F_1}{2}\beta(x). \tag{2.29}$$

Specifically the equivalent control is

$$\beta(x) = -\frac{H_x F_1 + H_x F_2}{H_x F_2 - H_x F_1}.$$

Filippov's method, by contrast, takes a simple convex combination of the two vector fields

$$F_{12} = (1 - \alpha)F_1 + \alpha F_2 \tag{2.30}$$

with $0 \leq \alpha \leq 1$, where

$$\alpha(x) = \frac{H_x F_1}{H_x(F_1 - F_2)}. \tag{2.31}$$

Sometimes, where there is no ambiguity, we shall write

$$F_{ij} := F_s$$

to represent the sliding vector field

Now it is a simple exercise to show that the above two methods are algebraically equivalent with $\beta = 2\alpha - 1$. (Note though that as shown in [257] there are some special cases where the two methodologies lead to subtly different results.) In both cases it is straightforward to show that the vector field F_s lies orthogonal to the direction H_x and so lies tangent to Σ. Utkin's method has the interpretation that β is precisely the control power that is needed to pull the flow back to being in a direction that is tangent to Σ; see Fig. 2.17(a). Another interpretation, from Filippov's method, is that just the right convex combination of the vector fields needs to be taken for the resulting field F_s to lie in Σ; see Fig. 2.17(b). A final interpretation is obtainable by separating the boundary to regions S_1 and S_2 slightly, within a hysteresis loop; see Fig. 2.17(c). That is, an initial condition in S_1 is allowed to evolve under flow F_1 until penetrating a small distance ε into S_2, then evolves under F_2 until passing back through Σ to a distance ε on the other side. (Thinking of the central heating example introduced in the Introduction, this would be where the temperature threshold for switching on the boiler is slighter greater than that for switching it off.) Then we can consider α to be proportion of time that a trajectory spends in the region S_1, in the limit $\varepsilon \to 0$.

Returning to the perfect sliding case, if the control $\beta(x) = -1$ (equivalently $\alpha = 0$), then the flow must be governed by F_1 alone, which must by definition be tangent to Σ at such a point. Similarly, $\beta = 1$ ($\alpha = 1$) represents a tangency of the flow F_2 with Σ. Hence we can define the sliding region as

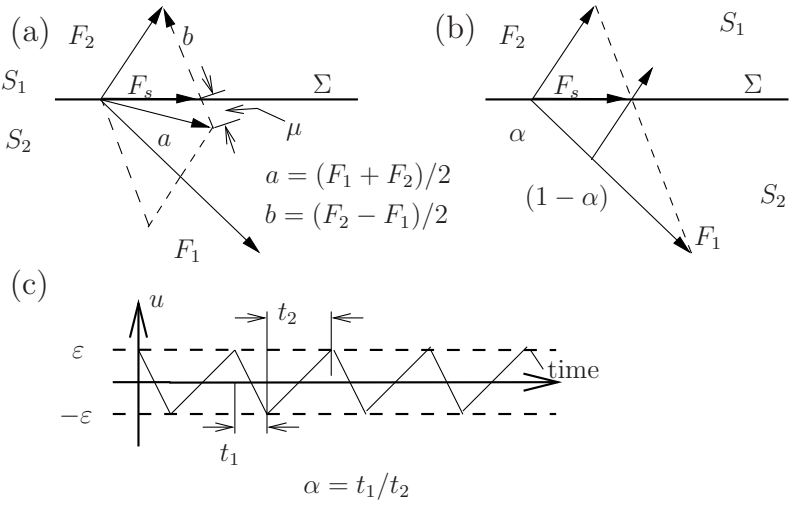

Fig. 2.17. The equivalent definitions of the sliding flow F_s, as defined in the text, illustrated in the two-dimensional case. In (c) the variable u is in the direction H_x orthogonal to Σ.

$$\widehat{\Sigma} := \{x \in \Sigma : -1 \leq \beta \leq 1\},$$

and the boundaries of the sliding region as

$$\partial\widehat{\Sigma}^{\pm} := \{x \in \Sigma : \beta = \pm 1\},$$

with tangency of one vector field or other occurring at the two different types of boundary.

2.2.4 Hybrid dynamical systems

Hybrid dynamical systems are combinations of maps and flows, giving rise to discontinuous, piecewise-smooth flows. They can arise both as models of impacting systems or in the context of the interaction between digital and analog systems. The notion of a *hybrid dynamical system* is a broad concept that encompasses a number of different formalisms in the literature. For example, *hybrid automata* [71, 183] are defined as dynamical systems with a discrete and a continuous part. The discrete dynamics can be represented as a graph whose vertices are the discrete states (or modes) and whose edges are transitions. The continuous states take values in $\mathbb{R}^n$ and evolve along trajectories, typically governed by ODEs or differential algebraic equations. The interaction between the discrete and the continuous dynamics takes place through *invariants* and *transition relations*. Each mode has an invariant associated with it, the violation of which as the system evolves says that a transition

must take place. The transition relations describe conditions on the continuous state that enable the transition to occur and also the effect (or reset) that the transition will have on the continuous state. This formalism is really quite broad and covers a wide variety of possible systems both physical and virtual, and in fact all the other formulations we describe in this chapter can be seen as just a special case. The drawback with such a general description is that it does not necessarily allow much general information to be gleaned, which applies to all systems of this class. For more details, see the book by Van der Schaft and Schumacher [71].

In this book we shall reserve the name 'hybrid' for a specific kind of piecewise-smooth system that comprises a collection of different smooth flows and maps; see Fig. 2.18

Definition 2.24. *A* **piecewise-smooth hybrid system** *comprises a set of ODEs*

$$\dot{x} = F_i(x, \mu), \quad \text{if} \quad x \in S_i, \tag{2.32}$$

plus a set of reset maps

$$x \mapsto R_{ij}(x, \mu), \quad \text{if} \quad x \in \Sigma_{ij} := \bar{S}_i \cap \bar{S}_j. \tag{2.33}$$

Here $\cup_i S_i = \mathcal{D} \subset \mathbb{R}^n$ *and each* S_i *has a non-empty interior. Each* Σ_{ij} *is either an* $\mathbb{R}^{(n-1)}$*-dimensional manifold included in the boundary* ∂S_j *and* ∂S_i*, or is the empty set. Each* F_i *and* R_{ij} *are assumed to be smooth and well defined in open neighborhoods around* S_i *and* Σ_{ij}*, respectively.*

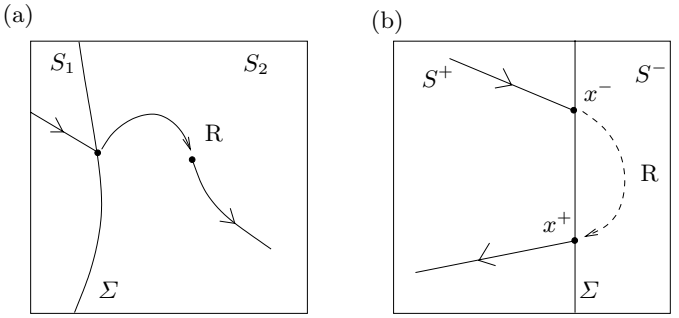

Fig. 2.18. (a) A hybrid system and (b) the impacting class of hybrid system.

In this book we will mostly study a special type of hybrid systems motivated by the impact oscillator example described in case study I. For such systems we generally consider surfaces Σ_{ij} that act as hard constraints, so that the reset R_{ij} maps the set Σ_{ij} back to itself.

Definition 2.25. *An* **impacting hybrid system** *is a piecewise-smooth hybrid system for which* $R_{ij} : \Sigma_{ij} \to \Sigma_{ij}$*, and the flow is constrained locally to lie on one side of the boundary; this is, in* $\overline{S}_i = S_i \cup \Sigma_{ij}$*.*

We shall often refer to the reset map R_{ij} in this context as being the *impact law* or *impact rule*. The discontinuity boundaries Σ_{ij} will be referred to as *impact surfaces* and the event of a trajectory intersecting Σ_{ij} as an *impacting event* or just an *impact*.

Throughout this book, we shall often consider a restrictive class of impacting hybrid systems that contain just one impact surface Σ. Suppose that such a surface Σ can be defined by the zero set of a smooth function $H(x)$,

$$\Sigma = \{x : H(x) = 0\}, \quad \text{and let} \quad S^+ = \{x : H(x) > 0\}, \tag{2.34}$$

with the dynamics constrained to the region S^+; see Fig. 2.19. Such systems can be thought of as describing the dynamics local to any impact surface in a general, multiple region system. Locally the dynamics may be written in the form

$$\dot{x} = F(x) \quad \text{if } H(x) > 0, \tag{2.35}$$

$$x \mapsto R(x) \quad \text{if } H(x) = 0, \tag{2.36}$$

for a smooth vector field F (which is well defined in a full neighborhood of Σ including for $H < 0$) and reset map R. Suppose an impact occurs at time t_0. Let x^- and x^+ represent the intersection of the flow with Σ both immediately before and immediately after the impact, so that $x^- = \lim_{t \to t_0^-}$, $x^+ = \lim_{t \to t_0^+}$. Hence we can write the impact surface as

$$x^+ = R(x^-). \tag{2.37}$$

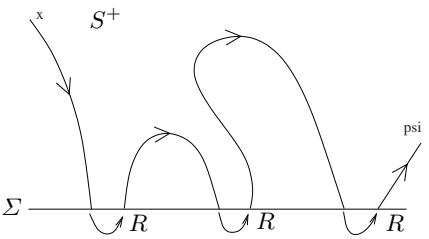

Fig. 2.19. The surface Σ and a multiple impacting trajectory for an impacting hybrid system with a single discontinuity boundary.

In order to be definite, we shall also assume a restrictive class of impact law that depends on the *normal velocity* $v(x)$ at which the trajectory approaches the impact manifold, given by

$$v(x) \equiv dH/dt = H_x F. \tag{2.38}$$

Specifically, we suppose that

$$R(x) = x + W(x)H_x F = x + W(x)v(x) \tag{2.39}$$

for a some smooth function $W(x) \in \mathbb{R}^n$. To motivate why (2.39) is a reasonable form to take, note that we would like an impact law that takes a grazing trajectory (one for which $v(x) = 0$) to itself and that is a smooth function of $v(x)$ otherwise. More complex forms of reset maps than (2.39) are required to deal with impacting mechanical systems with friction. For example, the so-called Painlevé paradox deals with mechanical systems that can both slide and impact; see, for example, [243, 174].

Given an impact rule of the form (2.39), the surface Σ can therefore be divided into three separate regions, Σ^-, Σ^+ and Σ^0 according to whether the normal velocity is, respectively, negative, positive or zero:

$$\begin{aligned} \Sigma^- = \{x \in \Sigma : v(x) < 0\}, \qquad & \Sigma^+ = \{x \in \Sigma : v(x) > 0\}, \\ \Sigma^0 \quad = \quad & \{x \in \Sigma : v(x) = 0\}. \end{aligned}$$

In general, if we write the impact law in the form (2.37), then we have $x^- \in \Sigma^-$ and $x^+ \in \Sigma^+$. In this case a flow in S^+ intersects Σ^-, is mapped to Σ^+ and then continues in S^+. The set Σ^0 is called the **grazing set**, and impacts close to it lead to subtle dynamics that we will analyze in detail in Chapter 6.

Example 2.7 (impact oscillator). Let us show that the impact oscillator with the simple coefficient of restitution law for impact, studied in case study I, fits into this framework. We can write the equations of motion (1.1) in the form

$$\begin{pmatrix} \dot{x}_1 \\ \dot{x}_2 \end{pmatrix} = \begin{pmatrix} 0 & 1 \\ -1 & -2\zeta \end{pmatrix} \begin{pmatrix} x_1 \\ x_2 \end{pmatrix} + \begin{pmatrix} 0 \\ \cos(\omega t) \end{pmatrix}, \tag{2.40}$$

together with the impact rule

$$\begin{pmatrix} x_1(t_j^+) \\ x_2(t_j^+) \end{pmatrix} = \begin{pmatrix} 1 & 0 \\ 0 & -1-r \end{pmatrix} \begin{pmatrix} x_1(t_j^-) \\ x_2(t_j^-) \end{pmatrix}, \tag{2.41}$$

which applies at times t_j for which $x_1 = \sigma$. Letting $x_3 = t$, we see that this fits into the above framework with $x = (x_1, x_2, x_3)^T$, $H = x_1 - \sigma$, $H_x F(x) = x_2$, and $W(x) = -(0, 1 + r, 0)^T$.

Many more examples of hybrid systems of this form will be given in Chapter 6, in which the detailed dynamics of hybrid systems and their bifurcations will be analyzed.

Let us now consider the basic flow of the simple impacting system (2.35)–(2.39). Starting from an initial condition $x(0) = x_0$ in S^+, the ODE (2.35) generates a smooth flow $\Phi(x_0, t)$ up until the flow strikes Σ, at time t_0, say. Suppose that this impact is *transversal*, so that the normal velocity $v(x(t_0)) < 0$. Hence $x^- = x(t_0) \in \Sigma^-$. This point is then mapped instantaneously under the action of the reset map to the point $x^+ = R(x^-)$. If $v(x^+) > 0$, so that $x^+ \in \Sigma^+$, then the flow moves away from Σ back into the set S^+ and is

described by the flow $\Phi(x^+, t)$. In principle, this scenario can repeat arbitrarily often, as illustrated in Figure 2.19.

However, this is not the only possible dynamics of the system. Consider a grazing point for which $v(x^-) = 0$, where the impact map becomes the identity. In order to understand what happens, it is useful to define the *normal acceleration* of the flow with respect to the boundary:

$$a(x) = d^2H/dt^2 = (H_xF)_xF = H_{xx}FF + H_xF_xF. \tag{2.42}$$

Now, in the case where $a(x^-) > 0$ at a grazing point, the curvature of the flow will cause the trajectory to immediately leave Σ. However, if $a(x) < 0$, then the flow will become **stuck** to the boundary, rather akin to the *sliding flow* of a Filippov system. Thus the **sticking subset** of the grazing set Σ^0 is determined by the conditions

$$\Sigma^0_- \equiv \{x : H(x) = 0, \quad v(x) = 0, \quad a(x) < 0\}.$$

The **sticking motion** evolves under the action of the vector field F, constrained to lie on the surface Σ. If we define the impact law according to (2.39), then it is possible to express the sticking vector field as

$$\dot{x} = F_s(x) = F(x) - \lambda(x)W(x), \tag{2.43}$$

where

$$\lambda(x) = \frac{a(x)}{(H_xF)_xW}. \tag{2.44}$$

To see that this corresponds to a sticking flow, note that in order to stick we require $H(x(t)) = v(x(t)) \equiv 0$. Differentiating the conditions $H(x) = 0$ and $v(x) = 0$ with respect to time, we have $H_x\dot{x} = 0$ and $v_x\dot{x} = 0$. The first of these conditions is satisfied identically when $H_xW = 0$, and the second condition if

$$0 = (H_xF)_xF - \lambda(H_xF)_xW = a(x) - \lambda(H_xF)_xW, \tag{2.45}$$

which defines λ according to (2.44). Note that (2.43)–(2.44) define a smooth flow $\Phi_s(x, t)$, which is also defined within a neighborhood of Σ, but for which the set $\Sigma\{x : H(x) = 0\}$ is invariant. For the hybrid system, the sticking flow ceases to apply when the trajectory leaves Σ^0_-. At such a point $a(x) = 0$, but $\frac{da(x)}{dt} := a_x(x)\dot{x} > 0$ and hence the system moves into S^+ where the original flow Φ applies. The condition that the vector field remains in the sticking region is $\lambda(x) > 0$. The formalism of complementarity systems described in the next section helps us understand the role played by this extra variable λ.

Typically, unlike the sliding motion in Filippov systems, impacting systems do not enter a sticking region directly, but via a **chattering sequence** (also known in control theory as a *Zeno phenomenon* [145]). Such a sequence begins if an impact occurs within Σ^-, close to the set Σ^0 with $v(x^+) \ll 1$ and

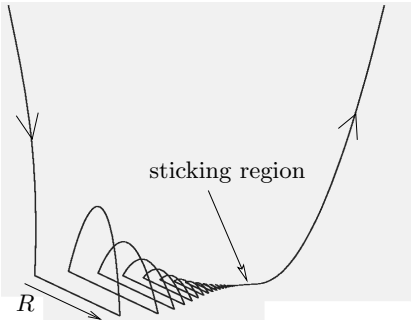

Fig. 2.20. A chattering sequence followed by sticking and release.

$a(x^+) < 0$; see Fig. 2.20. There follows an infinite sequence of impacts, of successively reduced velocity, which converges in *finite time*, onto a point in the sticking set [42, 203]. After the accumulation of such a sequence, the motion will evolve in the sticking set in the manner described above. We shall return to an analysis of chattering in Chapter 6. Chattering sequences are a commonly observed feature of hybrid systems and require special care when computing the flow numerically.

Hybrid systems, then, generally have state jumps. This should be contrasted with Filippov systems that have jumps in the vector field (time derivative of the flow) and piecewise-smooth continuous systems that have jumps in the second or higher derivative of the flow. Thus we can extend the notion of degree of smoothness in Definition 2.21 to say:

Definition 2.26. *A hybrid dynamical system that undergoes a jump in the system state* $\Phi(x,t) \mapsto R_{ij}(\Phi(x,t))$ *on a discontinuity boundary* Σ_{ij} *is said to have* **degree of smoothness zero**.

2.3 Other formalisms for non-smooth systems

The choice of formalism we choose in this book is essentially to deal with piecewise-smooth maps or with piecewise-smooth systems that have integer degree of smoothness across each of its boundaries Σ_{ij}. However, there is no guarantee that such a formulation leads to existence or uniqueness of solutions in all circumstances. Let us therefore briefly present several other formalisms for which more mature analytic theory is available.

2.3.1 Complementarity systems

Complementarity dynamical systems formalize the notion of a mechanical system with unilateral constraints. Such systems can be written most simply

in the form of a differential algebraic equation plus inequality constraints (see for example the reviews by Brogliato and co-workers [38, 127] and references therein):

$$\dot{x} = f(x, \lambda), \tag{2.46}$$
$$g(x, w, \lambda) = 0, \tag{2.47}$$
$$0 \leq w \perp \lambda \geq 0, \tag{2.48}$$
$$\text{re-initialization rule } R \text{ for state } x. \tag{2.49}$$

Here $x \in \mathbb{R}^n$ is the system state, $g \in \mathbb{R}^m$ are a set of side relations, $\lambda \in \mathbb{R}^l$ is a so-called *slack variable* and $w \in \mathbb{R}^l$ is the corresponding signal or system output. The expression $w \perp \lambda$ means that the vector w is orthogonal to λ, whereas $\lambda, w \geq 0$ means that all components of λ and w are non-negative. Hence, if a component w_i is positive then the corresponding λ_i must be zero, and *vice versa*.

Let us consider the dynamics of a system written in the form (2.46)–(2.47). The set of m relations (2.47) implicitly defines the signal w in terms of the states and slack variables (often the relations can be written explicitly as $w = \tilde{g}(x, \lambda)$). The most important part of the system is the orthogonality (or '*complementarity*') relation (2.48). This should be understood componentwise. That is, for each i, *either* λ_i is zero and w_i is non-negative *or* λ_i is positive and w_i is zero. At transition points, that is at times t_j for which $\lambda_i(t_j)$ and $w_i(t_j)$ are both zero for some $i \leq m$, then one in general has to apply a rule (2.49) to reset the state $x(t_j^+) = R(x(t_j^-), w, \lambda)$. Complementarity systems may be seen as a special case of hybrid automata, where the discrete states are the λ_i, the particular set of w_i that are non-zero describe the invariants, and the state re-initialization rule (and choice of new set of non-zero w_i) gives the transition relations.

Example 2.8 (impact oscillator). We illustrate the complementarity framework with the impact oscillator, case study I, which can be written in the complementarity form

$$\begin{aligned}
&\begin{pmatrix} \dot{x}_1 \\ \dot{x}_2 \end{pmatrix} = \begin{pmatrix} 0 & 1 \\ -1 & -2\zeta \end{pmatrix} \begin{pmatrix} x_1 \\ x_2 \end{pmatrix} + \begin{pmatrix} 0 \\ \cos(\omega t) + \lambda \end{pmatrix}, \\
&w = x_1 - \sigma, \\
&0 \leq w \perp \lambda \geq 0, \\
&\begin{pmatrix} x_1(t_j^+) \\ x_2(t_j^+) \end{pmatrix} = \begin{pmatrix} 1 & 0 \\ 0 & -1 - r \end{pmatrix} \begin{pmatrix} x_1(t_j^-) \\ x_2(t_j^-) \end{pmatrix}.
\end{aligned} \tag{2.50}$$

For this example, there are two kinds of motion (active modes): *free motion* of the oscillator where $\lambda = 0$ and $w > 0$, which implies that $x_1 > \sigma$; and *sticking motion* where $\lambda > 0$ and $w = 0$; hence, $x_1 = \sigma$. Here, the slack variable λ should be interpreted as a *Lagrange multiplier*, namely the force being exerted by the obstacle on the particle to stop it from penetrating. Clearly if this force

became negative, then the particle would be pulled into the obstacle; hence the requirement that $\lambda \geq 0$. In fact, it is possible to calculate explicitly the value that λ must take. Suppose that the particle is instantaneously in contact with the obstacle at some time τ. Then $x_1(\tau) = \sigma$. If it is to remain in contact, then we require that $x_1(t) \equiv \sigma$ for some time interval $t \in (\tau, \tau + \varepsilon)$. Hence $\dot{x}_1(\tau) = 0$ and $\ddot{x}_1(\tau) = 0$ also. The first of these conditions gives $x_2(\tau) = 0$, and the second gives

$$\lambda = \sigma - \cos(\omega t). \tag{2.51}$$

Hence, sticking motion can only occur for t-values such that $\cos(\omega t) < \sigma$.

In order to describe the motion completely we need to consider the transition times t_j when both λ and w are zero. Suppose first that the system is in free motion at t_j^- and reaches the constraint $x_1 = \sigma$. Then $w = 0$. Here, we apply the reset rule (2.50), which is just Newton's restitution law. Now, exceptions arise when the velocity $x_2 = 0$ at the impact point, so that grazing occurs. Then we have to look at the sign of $\dot{x}_2 = \cos(\omega t_j^-) - \sigma$. If this is positive, then we have a grazing trajectory, which immediately passes back into free motion again, since the reset rule gives $\dot{x}_1(t_j^+) = x_2(t_j^+) = 0$ but $\ddot{x}_1(t_j^+) = \dot{x}_2(t_j^+) > 0$ and so $x_1 > \sigma$ for $t = t_j + \varepsilon$ for some $\varepsilon < 0$. However, if $\dot{x}_2 < 0$, then a sticking motion ensues with a non-zero value of λ. As we have described above, the sticking region can only be entered after an infinite sequence of impacts (a chattering sequence). In contrast, the exit boundary from the sticking region is given by a zero of λ defined by (2.51). Hence, at this point we have that the first three time derivatives of x_1 are zero, but $\frac{d^3}{dt^3} x_1(t) = -\omega \sin(\omega t)$, which if negative implies that we are once again in the regime of free motion for small subsequent times. (In practice, this quantity will always be negative since the particle enters the sticking region at some time t such that $\cos(\omega t) < \sigma$ and leaves it at the first *later* time at which $\cos(\omega t) = \sigma$. Hence the angle ωt must be in the third or fourth quadrant, depending on whether $\sigma > 0$ or $\sigma < 0$. Hence $\sin(\omega t)$ must be positive.)

We can generalize this example by putting any piecewise-smooth ODE system into complementarity form, at least local to a single discontinuity boundary. For piecewise-smooth continuous systems in a neighborhood of a single uniformly discontinuous boundary, where $F_1(x, \mu) - F_2(x, \mu)$ is of the form (2.28), a corresponding complementarity formulation of (2.27) is

$$\begin{cases} \dot{x} = F_1(x, \mu) + \lambda^{m-1} J(x, \mu), \quad w = -H(x, \mu) + \lambda, \\ 0 \leq w \perp \lambda \geq 0, \end{cases} \tag{2.52}$$

for which there is no need for a reset rule. Table 2.1 shows the possible active modes of motion of the system.

In the Filippov case, i.e., for systems with degree of smoothness one, a different form of complementarity formulation is required. For example, given a two-zone system (2.27) with a single discontinuity boundary, we have

Table 2.1. The different possible active modes for the dynamics of the piecewise-smooth continuous ODE (2.52).

w and λ	dynamical system
$w = 0, \lambda > 0$	$\dot{x} = F_2 = F_1(x,\mu) + H(x,\mu)^{m-1} J(x,\mu)$
$w > 0, \lambda = 0$	$\dot{x} = F_1(x,\mu)$
$w = 0, \lambda = 0$	$\dot{x} = F_1(x,\mu)$ and $H(x,\mu) = 0$

$$\begin{cases} \dot{x} = F_1(x,\mu) + \lambda_1(F_2(x,\mu) - F_1(x,\mu)), \\ w_1 = -H(x,\mu) + \lambda_2, \\ w_2 = 1 - \lambda_1, \\ 0 \le w_1 \perp \lambda_1 \ge 0, \\ 0 \le w_2 \perp \lambda_2 \ge 0. \end{cases} \tag{2.53}$$

Table 2.2 gives the different possible dynamical regimes of such systems.

Table 2.2. The different possible active modes for the dynamics of the Filippov system (2.53).

C1	C2	dynamical system
$w_1 = 0,\ \lambda_1 = 1$	$w_2 = 0,\ \lambda_2 \ge 0$	$\dot{x} = F_2(x,\mu)$
$w_1 \ge 0,\ \lambda_1 = 0$	$w_2 = 1,\ \lambda_2 = 0$	$\dot{x} = F_1(x,\mu)$
$w_1 = 0,\ 0 \le \lambda_1 \le 1$	$0 \le w_2 \le 1,\ \lambda_2 = 0$	$\dot{x} = F_1(x,\mu) + \lambda_1(F_2(x,\mu) - F_1(x,\mu))$ $H(x,\mu) = 0$

Notice that the concept of the sliding vector field is embedded in the complementarity description of the system of interest. In fact, in the third case in Table 2.2, the dynamical system is a convex combination of the two original vector fields. The parameter λ_1 can be calculated directly from the requirement that $H(x,\mu) \equiv 0$ along such solutions. Hence

$$\frac{dH}{dt}(x,\mu) := H_x(x,\mu)\,[F_1(x,\mu) + \lambda_1(F_2(x,\mu) - F_1(x,\mu))] = 0. \tag{2.54}$$

Thus

$$\lambda_1 = \frac{H_x F_1}{H_x F_1 - H_x F_2},$$

which is the parameter α in Filippov's convex method introduced in (2.30). There thus seems an advantage of the complementarity framework over the piecewise-smooth one in this case. Checking the slack variables will automatically detect when sliding is occurring and when the sliding region is exited. That we had to differentiate the constraint once to obtain λ_1 means that the constraint and the differential equation have *relative degree one*. Equivalently the sliding mode of the complementarity system is an *index 1* differential algebraic equation (DAE). Note, in contrast, that the complementarity

formulation for piecewise-smooth continuous systems (2.52) does not require differentiation of the constraint, since λ is given explicitly. Thus the constraint has relative degree zero, and the mode when $w = 0$ is a DAE with index 0, which is equivalent to just an ODE.

Finally, consider a hybrid system with a single impact boundary for which the reset map is written in the form (2.39). This can be written as the complementarity system

$$\begin{cases} \dot{x} = F(x,\mu) - \lambda W(x,\mu), \\ w = H(x,\mu), \\ 0 \le w \perp \lambda \ge 0, \\ x(t^+) = x(t^-) + W(x(t^-),\mu) H_x F(x(t^-),\mu), \end{cases} \tag{2.55}$$

which is a generalization of the complementarity framework for the impact oscillator (2.50). Note that this has relative degree two in the sticking mode, since the value for λ is obtained by differentiating the constraint $H(x) = 0$ twice with respect to t.

The complementarity framework is not just restricted to problems with single discontinuity boundaries. In principle each of the above kinds of constraints and corresponding slack variables can be concatenated to take account of multiple boundaries.

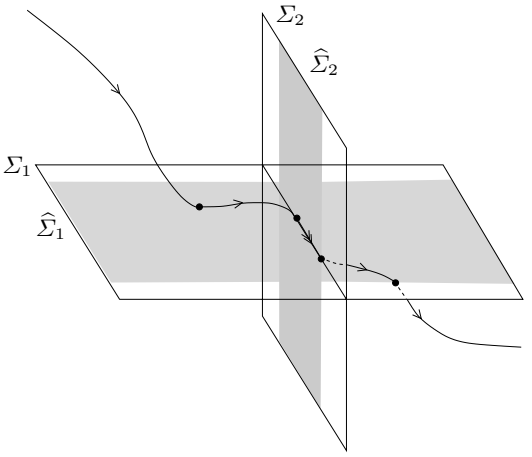

Fig. 2.21. Higher-order sliding occurring when two sliding regions $\widehat{\Sigma}_1$ and $\widehat{\Sigma}_2$ intersect.

For example, suppose a piecewise-smooth system is written in the form

$$\dot{x} = \begin{cases} F_1(x), & \text{if } H_1(x) > 0, \ H_2(x) > 0, \\ F_2(x), & \text{if } H_1(x) > 0, \ H_2(x) < 0, \\ F_3(x), & \text{if } H_1(x) < 0, \ H_2(x) > 0, \\ F_4(x), & \text{if } H_1(x) < 0, \ H_2(x) < 0; \end{cases}$$

see Fig. 2.21. This can be rewritten as the following complementarity system:

$$\dot{x} = \lambda_1\lambda_2 F_1(x) + \lambda_1(1-\lambda_2)F_2(x) + (1-\lambda_1)\lambda_2 F_3(x) + (1-\lambda_1)(1-\lambda_2)F_4(x), \tag{2.56}$$

$$\begin{cases} w_1 = -H_1(x,\mu) + \lambda_3, & w_2 = -H_2(x,\mu) + \lambda_4, \\ w_3 = 1-\lambda_1, & w_4 = 1-\lambda_2, \\ 0 \le w_1 \perp \lambda_1 \ge 0, & 0 \le w_2 \perp \lambda_2 \ge 0, \\ 0 \le w_3 \perp \lambda_3 \ge 0, & 0 \le w_4 \perp \lambda_4 \ge 0. \end{cases} \tag{2.57}$$

The most interesting case is when both w_1 and w_2 are zero, whereas w_3 and w_4 are both positive. Then, according to (2.57), we have $0 < \lambda_1 < 1$ and $0 < \lambda_2 < 1$ and the motion is constrained to a codimension-two set $\{H_1(x) = H_2(x) = 0\}$. The flow on this set we refer to as *higher-order sliding*, which we shall return to in Chapter 8, and is given by (2.56), where λ_1 and λ_2 are obtained from the pair of simultaneous equations that arise from differentiation of the constraints

$$\begin{aligned} H_{1x}\left[\lambda_1\lambda_2 F_1 + \lambda_1(1-\lambda_2)F_2 + (1-\lambda_1)\lambda_2 F_3 + (1-\lambda_1)(1-\lambda_2)F_4\right] = 0, \\ H_{2x}\left[\lambda_1\lambda_2 F_1 + \lambda_1(1-\lambda_2)F_2 + (1-\lambda_1)\lambda_2 F_3 + (1-\lambda_1)(1-\lambda_2)F_4\right] = 0. \end{aligned}$$

Once the problem has been formulated in the complementarity framework, it is possible to study its well-posedness using the analytic tools developed for unilaterally constrained optimization; see, for example, [40] for an extensive review. For example, any complementarity systems for which we can write

$$w = G(x) + D\lambda$$

for a smooth function G and invertible matrix D, is equivalent to a set of ODEs with degree of smoothness at least 1. If the matrix D is a so-called P-matrix (i.e., a matrix with positive principal minors), then it can be shown that the corresponding complementarity problem has a unique solution. This means that systems such as (2.52) where $D = 1$ and $G = H(x,\mu)$ have a unique solution for all parameter values μ.

Complementarity systems are also useful because they provide a general framework for describing systems with more than one (perhaps many thousands) of constraints. They come armed with a set of numerical solution techniques, that do not require the precise detection of the events t_j, where λ_i and w_i are both zero; see [41] for a review.

2.3.2 Differential inclusions

Another way of putting piecewise-smooth systems on a rigorous footing is to use a variational formulation. We shall not go into details, but the key notion is that of a *differential inclusion*. Here we allow the right-hand side of an ordinary differential equation $\dot{x} = f(x)$ to be not strictly a function (that is, returning a single value $f(x)$ for each x), but to be set-valued. For example,

such set-valued functions arise in Coulomb dry friction laws encountered in mechanics. Specifically, Coulomb friction models objects in contact that slip over each other with velocity v only if their tangential contact force f_t exceeds some critical value. The function

$$f_t = C(v) = \alpha_0 \mathrm{sgn}(v) - \alpha_1(v) + \alpha_2(v)^3 \tag{2.58}$$

occurring in case study IV is an example of such a law, see Fig. 2.22(a). The problem with (2.58) is that it does not specify what value f_t should take at $v = 0$. Using the notion of a differential inclusion, we rewrite f_t as a set-valued function

$$f_t(v) = \begin{cases} \{[-\alpha_0, \alpha_0]\}, & \text{if} \quad v = 0, \\ \alpha_0 \mathrm{sgn}(v) - \alpha_1 v + \alpha_2 v^3, & \text{otherwise.} \end{cases}$$

So now, instead of $\ddot{y} + y = f_t(1 - \dot{y}) + a\cos(\nu t)$, we write

$$\ddot{y} + y - a\cos(\nu t) \in f_t(1 - \dot{y}),$$

because at $\dot{y} = 1$, f_t can take on a range of values. In [69], Deimling explains that to obtain a well-posed problem, one has to 'fill in' the gap between $[-\alpha_0, \alpha_0]$ at $v = 0$ (i.e., perform a so-called *convexification* of the problem).

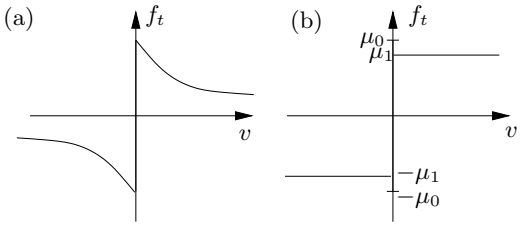

Fig. 2.22. Two idealized Coulomb friction characteristics showing the tangential force f_t as a function of velocity v.

In general, any Filippov system can be written as a differential inclusion. For example, a two-zone system can be written as

$$\dot{x} \in f(x), \quad \text{where} \quad f = \begin{cases} \{F_1(x)\}, & \text{if} \quad H(x) > 0, \\ \{F_2(x)\}, & \text{if} \quad H(x) < 0, \\ \{F_1(x) + \alpha(F_2 - F_1) | 0 \le \alpha \le 1\}, & \text{if} \quad H(x) = 0. \end{cases}$$

The concept of the inclusion is especially useful when we take more general Coulomb friction laws like the one in Fig. 2.22(b), where the static coefficient of friction is different from the dynamic one:

$$f_t(v) = \begin{cases} [-\mu_0, \mu_0], & \text{if} \quad v = 0, \\ \{\mu_1 \mathrm{sgn}(v)\}, & \text{otherwise.} \end{cases}$$

In cases where the right-hand side $f(x)$ of an inclusion $\dot{x} \in f(x)$ satisfies some quite general properties (f is upper semi-continuous, non-empty, convex and compact for all x, and is bounded by an affine function of x), then there is a general theory that gives the existence of absolutely continuous solutions [69]. Unfortunately, many non-smooth systems when put into an inclusion form do not satisfy these hypotheses.

Example 2.9 (Lagrangian systems). Another way of writing a general impacting mechanical system in differential inclusion form is to use a Lagrangian approach. This leads to a second-order ODE system for generalized co-ordinates $q \in \mathbb{R}^n$. Consider such a system with mass matrix $M(q)$ and generalized non-contact forces $F(q, \dot{q}, t)$, in the absence of damping, that is constrained to the region of configuration space $S = \{h(q) \geq 0\}$. Its dynamics may be written as

$$M(q)\ddot{q} + F(\dot{q}, q, t) \in \partial\psi_S(q), \text{ if} \quad t \neq t_k, \tag{2.59}$$

$$\dot{q}(t_k^+) = R(\dot{q}(t_k^-)), \text{ if} \quad t = t_k, \tag{2.60}$$

where the $\{t_k, k = 1, 2, 3 \ldots\}$ are the *a priori* unknown set of impact times where $q \in \Sigma = \{h = 0\}$, and R is a reset rule. Here $\partial\phi(q)$ represents the *sub-differential* (the set of all possible one-sided limits $\lim_{t\to 0} \frac{\phi(q+tv)-\phi(q)}{t}$ for any vector v) and ψ_{S_1} is the *indicator function* of the set S_1, which is 0 for all points inside S_1 and infinite outside. Thus $\partial\psi_{S_1}$ is the empty set for all points outside S_1, is equal to the *normal cone* $N_K(x) = \{z | z \cdot (x - z) = 0$, for all $z \in S_1\}$ inside the boundary $\Sigma = \partial S$, and is 0 for points in the interior of S. This set is not compact, and so the general existence theory does not apply. A particular form of reset map R (corresponding to coefficient of restitution 0) is the so-called Moreau collision mapping that the velocity $\dot{q}(t_k^+)$ is in the so-called *polar cone* $V(q)$ for $q \in \Sigma$. Here $V(x) = \{z | z \cdot x \leq 0$, for all $x \in N_K(x)\}$, with the additional constraint that the jump in kinetic energy is minimized.

A way of dealing more generally with systems that have state jumps is via the formalism of *measure differential inclusions* introduced by Schatzman [230] and Moreau [192]. This is motivated by the idea that one would like a framework that allows the velocity jumps at impacts to be included explicitly in the differential equation.

Example 2.10 (impact oscillator without damping).

$$\ddot{u} = -u + f(t), \quad u > \sigma, \quad \text{plus the impact law.}$$

It is tempting to integrate, and write formally

$$\int \mathrm{d}\dot{u} = \int (-u + f(t))\mathrm{d}t + \int \mathrm{d}R(u),$$

where $\mathrm{d}R$ is a *measure* that is zero at all times other than t_k and gives the value of the jump in $\dot{u}$ at impact. This leads to a general formulation where

one defines a measure $\mathrm{d}\mu = \mathrm{d}t + \Sigma_{k\geq 0}\delta(t_k)$, where $\delta(x)$ is the Dirac δ function, and we write

$$\frac{\mathrm{d}\dot{u}}{\mathrm{d}\mu} + (u - f(t))\frac{\mathrm{d}t}{\mathrm{d}\mu} \in F(u,t),$$

where

$$F(u,t) = \begin{cases} \{0\}, & \text{if} \quad t \neq t_k, \\ [0,\infty], & \text{if} \quad t = t_k. \end{cases}$$

Here we have introduced an example of a measure differential inclusion, which more generally can be written in the form

$$\frac{\mathrm{d}x}{\mathrm{d}\mu} + g(x(t^+),t^+)\frac{\mathrm{d}t}{\mathrm{d}\mu} \in F(x(t^+),t^+),$$

where μ is a positive measure on the time axis, and the set-valued function $F(x,t)$ satisfies the properties of being a cone for all x and t. The more general multi-degree-of-freedom mechanical system (2.59), (2.60) with impacts can also be put in this framework, upon writing

$$-M(q(t))\frac{\mathrm{d}\dot{q}}{\mathrm{d}\mu} - F(q(t),v(t))\frac{\mathrm{d}\dot{t}}{\mathrm{d}\mu} \in \partial\psi_{V(q(t))(\dot{q}(t^+)} \subseteq \partial\Psi_S\left(g(t)\right),$$

which is an example of a so-called *Moreau sweeping process*; see [166].

Many things can be proved about the dynamics of each of many subtly different classes of differential inclusions (either in measure form or not). They also have use in that they suggest natural ways to define numerical algorithms that preserve the properties of the inclusion that can be proved theoretically. However, we shall ignore such mathematical technicalities in this book and stick to a more pragmatic approach.

2.3.3 Control systems

Many concepts in non-smooth dynamical systems have a counterpart (often with different notation) in control theory. There, the goal is often to prove stability of some target state (such as an equilibrium point), or to design control laws in order to achieve such stability. See for example [240, 179, 255]. This book takes a rather different emphasis, which is to gain a qualitative understanding of complex dynamics via the (discontinuity-induced) transitions that can occur upon varying a parameter. It is nevertheless useful to spell out links with some of the ideas that arise in the control theory literature. For simplicity, we stick to the case of single-input single-output (SISO) systems. Here, the concept of *relative degree* is important; with the term having a rather different meaning to its use in complementarity systems, but nevertheless having a close link to our concept of degree of smoothness.

Consider a SISO linear system [240] given by

$$\begin{aligned} \dot{x} &= Ax + Bu, \\ y &= C^T x + Du. \end{aligned} \tag{2.61}$$

Here $x(t) \in \mathbb{R}^n$ is the *state vector*, $u(t) \in \mathbb{R}$ the *control input* and $y(t) \in \mathbb{R}$ the *output* of the system.

Definition 2.27. *The* **relative degree** *of the SISO linear control system (2.61) can be defined in terms of* **Markov parameters**

$$(M_0, M_1, M_2, M_3, \ldots) := (D, C^T B, C^T AB, C^T A^2 B, \ldots)$$

as the first index i for which M_i is nonzero.

Now it is easy to see how this concept is closely related to the degree of smoothness introduced in Definition 2.21. Take a relay control system, case study III, as a representative example. The system can be written as

$$\begin{aligned} \dot{x} &= Ax + Bu, \\ y &= C^T x + Du, \\ u &= -\mathrm{sgn}(C^T x). \end{aligned} \tag{2.62}$$

Then, according to Definition 2.27, this system has *relative degree 0* provided $D \neq 0$. In this case the discontinuity of the input u is translated into a discontinuity of the output y. Thus the relative degree is equal to one less than the degree of smoothness defined by Definition 2.21.

If instead $D = 0$ but $C^T B \neq 0$ in (2.62), then the *relative degree* is 1 and the output y is continuous but

$$\dot{y} = C^T \dot{x} = C^T Ax + C^T Bu$$

is discontinuous. Again the relative degree is one less than the degree of smoothness, which is 2 since the first derivative is the lowest differential of the state y having discontinuity. Similarly, if $D = 0$, $C^T B = 0$ but $C^T AB \neq 0$, then (2.62) has relative degree two because y and $\dot{y}$ are continuous, but

$$\ddot{y} = C^T \ddot{x} = C^T A^2 x + C^T ABu$$

is discontinuous. That is, the second derivative of the output is now discontinuous and the degree of smoothness is thus three.

These concepts extend to nonlinear control systems too. A general single-input single-output nonlinear system can be written as

$$\begin{aligned} \dot{x} &= f(x) + g(x)u, \\ y &= h(x). \end{aligned} \tag{2.63}$$

The system (2.63) is said to have *relative degree* r at a point x^* if

1. $\mathcal{L}_g \mathcal{L}_f^k h(x) = 0$ for all x in a neighborhood of x^* and all $k < r - 1$;
2. $\mathcal{L}_g \mathcal{L}_f^{r-1} h(x^*) \neq 0$.

Here we have introduced the following useful notation

Definition 2.28. *The* **Lie derivative** $\mathcal{L}_f$ *is the total time derivative along the direction of the flow governed by vector field* f*. Specifically, if* $f(x)$ *and* $g(x)$ *are smooth vector fields and* $h(x)$ *is a smooth scalar function, then we have*

$$\begin{aligned}\mathcal{L}_f h(x) &:= \frac{\partial h}{\partial x} f(x),\\ \mathcal{L}_g \mathcal{L}_f h(x) &:= \frac{\partial (\mathcal{L}_f h)}{\partial x} g(x),\\ \mathcal{L}_g \mathcal{L}_f^k h(x) &:= \frac{\partial (\mathcal{L}_f^{k-1} h)}{\partial x} g(x),\\ \mathcal{L}_f^0 h(x) &:= h(x).\end{aligned}$$

Consider, for example, a case where the relative degree is two at a point x^*. Here $r = 2$ and $k < 1$, which gives

$$\begin{aligned}&\mathcal{L}_g \mathcal{L}_f^0 h(x) = \tfrac{\partial (\mathcal{L}_f^0 h)}{\partial x} g(x) = h_x g(x) = 0,\\ &\mathcal{L}_g \mathcal{L}_f^1 h(x^*) = \tfrac{\partial (\mathcal{L}_f^1 h)}{\partial x} g(x^*) = \tfrac{\partial (h_x f)}{\partial x} g(x^*) = (h_{xx} f + h_x f_x) g(x^*) \neq 0;\end{aligned}$$

or, showing the link to the linear SISO system (2.61)

$$\begin{aligned}&\mathcal{L}_g \mathcal{L}_f^0 h(x) = h_x g(x) = AB = 0,\\ &\mathcal{L}_g \mathcal{L}_f^1 h(x^*) = (h_{xx} f + h_x f_x) g(x^*) = (0Ax^* + C^T A)B = C^T AB \neq 0,\end{aligned}$$

where $Ax = f(x)$, $B = g(x)$ and $C^T x = h(x)$.

The Lie derivative will prove useful in Chapters 6, 7 and 8 for analyzing the flow near to grazing intersections. At various points in the book, we will borrow other concepts from control theory, where it is useful, such as observer canonical form, controllability and relay control.

2.4 Stability and bifurcation of non-smooth systems

The extension of well-established concepts for smooth systems to the case of non-smooth systems is still an open research area. We shall hence try to establish a pragmatic approach for studying the asymptotic and structural stability of our chosen classes of piecewise-smooth maps, flows and hybrid systems (Definitions 2.18, 2.20 and 2.24). Our aim is to come up with a utilitarian definition of a discontinuity-induced bifurcation (DIB) that allows us to explain the dynamical transitions that were observed in the case study examples introduced in Chapter 1. First we need to assess the notion of stability.

2.4.1 Asymptotic stability

It is a particularly cumbersome task to provide necessary and sufficient conditions that guarantee the asymptotic stability of an invariant set of a piecewise-smooth systems if that set straddles the boundary between two regions S_i and S_j; see, for example, [179] for a review. Even the problem of assessing the asymptotic stability of an equilibrium that rests on a discontinuity boundary is an open problem in general [36]. Let us focus on the problem for the special case of piecewise-linear systems, which will be of relevance to the material in Chapter 5.

Consider the piecewise-linear system

$$\dot{x} = \begin{cases} A^- x & \text{if } C^T x \leq 0 \\ A^+ x & \text{if } C^T x \geq 0 \end{cases}, \tag{2.64}$$

where $A^{\pm} \in \mathbb{R}^{n\times n}$ and $c \in \mathbb{R}^n$. We assume that the overall vector field is continuous across the hyperplane $\{x : C^T x = 0\}$, but the degree of smoothness is uniformly one. This means that

$$A^- - A^+ = EC^T,$$

for some $E \in \mathbb{R}^n$. For the planar case, i.e., $n = 2$, a complete theory is possible and it can be shown that the equilibrium point $x = 0$ of (2.64) is asymptotically stable under certain strict conditions, provided the system obeys the property of *observability* often used in control theory.

Definition 2.29. *Two matrices $A \in \mathbb{R}^{n\times n}$ and $C^T \in \mathbb{R}^{p\times n}$ are said to be* **observable** *if the observability matrix, $\mathcal{O}$, defined as*

$$\mathcal{O} = \begin{pmatrix} C^T \\ C^T A \\ \vdots \\ C^T A^{n-1} \end{pmatrix}$$

has full rank. Equivalently, for single-output systems, where $V \in \mathbb{R}^{1\times n}$, observability implies $det(\mathcal{O}) \neq 0$.

Theorem 2.6 ([49]). *Consider the system (2.64) with $n = 2$. Assume that the pair (C^T, A^-) is observable. Then*

1. *The origin is asymptotically stable if and only if*
   a) neither A^- nor A^+ has a real non-negative eigenvalue, and
   b) if both A^- and A^+ have non-real eigenvalues, then $\sigma^-/\omega^- + \sigma^+/\omega^+ < 0$, where $\sigma^{\pm} \pm i\omega^{\pm}$ $(\omega^{\pm} > 0)$ are the eigenvalues of $A^{\pm}$.
2. *The system (2.64) has a non-constant periodic solution if and only if both A^- and A^+ have non-real eigenvalues and $\sigma^-/\omega^- + \sigma^+/\omega^+ = 0$, where $\sigma^{\pm} \pm i\omega^{\pm}$ $(\omega^{\pm} > 0)$ are the eigenvalues of $A^{\pm}$. Moreover, if there is one periodic solution, then all other solutions are also periodic. Moreover any such periodic solution has period equal to $\pi/\omega^- + \pi/\omega^+$.*

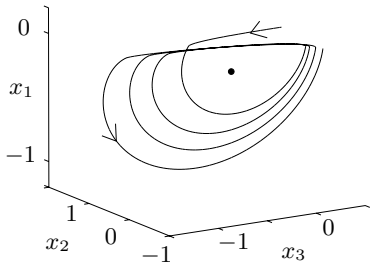

Fig. 2.23. A trajectory of the piecewise-linear system (2.64)–(2.66).

In higher dimensions, the problem becomes considerably more difficult. A seemingly paradoxical situation can occur whereby the origin of the individual systems $\dot{x} = A^- x$ and $\dot{x} = A^+ x$ is asymptotically stable, but is unstable for the combined system (2.64):

Example 2.11 (Unstable piecewise-linear system [51]). Consider the system (2.64) with

$$A^- = \begin{pmatrix} -1 & -1 & 0 \\ 1.28 & 0 & -1 \\ -0.624 & 0 & 0 \end{pmatrix}, \quad A^+ = \begin{pmatrix} -3.2 & -1 & 0 \\ 25.61 & 0 & -1 \\ -75.03 & 0 & 0 \end{pmatrix} \tag{2.65}$$

and

$$c = \begin{pmatrix} 1 \\ 0 \\ 0 \end{pmatrix}. \tag{2.66}$$

Now, the eigenvalues of A^- are $-0.2 \pm i$ and -0.6, whereas the eigenvalues of A^+ are $-0.1 \pm 0.5i$ and -3. Both sets are strictly in the left half-plane which would imply stability of the origin of each linear systems individually. Yet the combined piecewise-linear system has trajectories that tend to ∞; see Fig. 2.23.

In essence, the paradox is caused by the geometric relationship between the *eigenvectors* of the matrices A^- and A^+. Clearly if the eigenvectors of the two matrices were perfectly aligned, then stability of the matrices A^- and A^+ would be sufficient to establish stability of the piecewise-linear system. In fact, in certain other special cases, it is possible to establish conditions for stability for systems of the form (2.64) in three dimensions. For example, using the theory of invariant cones, Carmona *et al.* [51] have established the following result.

Theorem 2.7 ([51]). *Consider the system (2.64) with $n = 3$. Assume that the pair (C^T, A^-) is observable. Let $A^\pm$ and c be given by*

$$A^{\pm} = \begin{pmatrix} t^{\pm} & -1 & 0 \\ m^{\pm} & 0 & -1 \\ d^{\pm} & 0 & 0 \end{pmatrix}, \quad C = \begin{pmatrix} 1 \\ 0 \\ 0 \end{pmatrix}$$

(so-called observer canonical form). Suppose that the eigenvalues of the matrices $A^{\pm}$ *are* $\lambda^{\pm} \in \mathbb{R}$ *and* $\sigma^{\pm} \pm i\omega^{\pm}$*, where* $\omega^{\pm} > 0$*. Also, suppose that*

$$(\sigma^- - \lambda^-)(\sigma^+ - \lambda^+) < 0 \quad \textit{and} \quad (t^+ - t^-)(\sigma^+ - \lambda^+) \leq 0,$$

then the origin is an asymptotically stable equilibrium point if, and only if, $\lambda^{\pm}$ *are both negative.*

In the control theory literature, a more general tool has been proposed for the stability analysis of piecewise-smooth dynamical systems. Take, for example, the problem of establishing whether an equilibrium point in a discontinuity boundary of a piecewise-smooth dynamical system is asymptotically stable. One technique for proving such stability is to find a *common Lyapunov function*, that is, a function $V(x)$ that is *Lyapunov* (positive definite and decreasing along trajectories) for each of the vector fields defining the system dynamics in each of the phase space regions [179]. However, finding such functions in practice is at best difficult.

General progress toward understanding and classifying the dynamics of piecewise-smooth systems using such methods would appear hopeless. Drawing lessons from smooth dynamical systems theory, we advocate in this book a rather different approach. Instead of focusing on asymptotic stability of individual states or invariant sets, we focus instead on structural stability and bifurcation. Since *proving* stability from first principles can be hard, one should instead attempt to *classify* all the mechanisms that can lead to instability as a parameter is varied. Along with the classification should come techniques, both analytical and numerical, for identifying which case occurs in a particular example system and for understanding the nearby dynamics.

2.4.2 Structural stability and bifurcation

Consider a general invariant set of a piecewise-smooth dynamical system as defined in Definitions 2.18, 2.20 or 2.25. Bifurcations that involve invariant sets contained within a single region S_i for all parameter values of interest can be studied using smooth bifurcation theory. Also, it may be that the invariant set of a flow crosses several discontinuity boundaries, but nevertheless the Poincaré map associated with that invariant set is smooth. For example, in Sec. 2.5 below, we shall show that the Poincaré map associated with a periodic orbit that crosses all discontinuity sets Σ_{ij} transversally is smooth. Thus, *all the bifurcations discussed in Sec. 2.1.6 can also occur in piecewise-smooth systems.* However, other bifurcations are unique to piecewise-smooth systems. These typically involve non-generic interactions of an invariant set with a discontinuity boundary.

For piecewise-smooth systems such as (2.23) and (2.22) or (2.32) and (2.33), which define a dynamical system (this excludes the possibility of regions of phase space where there is repelling sliding or repelling sticking motion since this leads to no uniqueness in forward time), one can adopt the same notion of bifurcation as in Definition 2.16, applied to the entire system. However, we may wish to highlight other events that might not be a bifurcation of the entire system in this classical sense. In control systems for example, it may be important to identify whether a certain switch is activated. Or, in a mechanical system, we may need to know whether an attractor contains trajectories that impact or go beyond a certain threshold at which a bi-linear spring moves into its stiffer region. The transition that causes such an event will typically represent an invariant set forming a new crossing of a discontinuity boundary, as a parameter is varied. For example, at a parameter value $\mu = \mu_0$, a limit cycle of a piecewise-linear flow may become tangent to a discontinuity boundary Σ_{ij} at a *grazing point*. Alternatively, an equilibrium of a flow, or fixed point of a map, may approach a discontinuity boundary as $\mu \to \mu_0$. Now, if the degree of smoothness is sufficiently high, this will not affect the stability of these invariant sets and there will be no bifurcation in the sense of Definition 2.16. In the Russian literature, (e.g., [95, 98]), the term *C-bifurcation* has been adopted for such transitions that involve an invariant set doing something structurally unstable with respect to a discontinuity boundary. (The Russian character C, pronounced "S", stands for sewing, as one *sews* together two different trajectory segments on either side of the discontinuity boundary.) When the invariant set is the fixed point of a map, these have also been termed *border-collision bifurcations* [205].

Here we shall introduce the broader concept of a *discontinuity-induced bifurcation* [64, 79]. By this term we will identify qualitative changes to the topology of invariant sets with respect to the discontinuity boundaries. Specifically, we wish to single out parameter values at which the invariant set changes its *event sequence*; that is, the order and sense of interaction with the discontinuity boundaries. Such changes are typically brought about (or induced) through non-transversal interaction with a discontinuity boundary. However, in keeping with the qualitative theory of dynamical systems, we should like a definition of a discontinuity-induced bifurcation that is purely topological and does not refer to individual trajectories or invariant set. In order to come up with such a notion, we will need new definitions of structural stability and topological equivalence that call two dynamical systems non-equivalent if key invariant sets in the dynamics change their event sequence. We shall state this new definition of equivalence in the case of a hybrid dynamical system; corresponding definitions for piecewise-smooth maps and flows follow in an obvious manner.

Definition 2.30. *Let* $\{T, \mathbb{R}^n, \phi^t\}$ *and* $\{T, \mathbb{R}^n, \tilde{\phi}^t\}$ *be two hybrid piecewise-smooth dynamical systems (2.32), (2.33) defined by countably many different smooth flows* $\phi_i(x,t)$ *and* $\tilde{\phi}_i(x,t)$ *in finitely many phase space regions* S_i

and $\tilde{S}_i$*, respectively,* $i = 1 \dots N$*, with smooth resets* R_{ij} *and* $\tilde{R}_{ij}$ *applying, respectively, at each non-empty discontinuity boundaries* Σ_{ij} *and* $\tilde{\Sigma}_{ij}$*.*

Two such piecewise-smooth systems are called **piecewise-topological equivalent** *if:*

1. *They are topological equivalent; that is, there is a homeomorphism* h *that maps the orbits of the first system onto orbits of the second one, preserving the direction of time so that* $\phi^t(x) = h^{-1}(\tilde{\phi}^s(h(x)))$ *where the map* $t \to s(t)$ *is continuous and invertible.*
2. *The homeomorphism* h *can be chosen so as to preserves each of the discontinuity boundaries. That is, for each* i *and* j*,* $h(\Sigma_{ij}) = \tilde{\Sigma}_{ij}$*.*

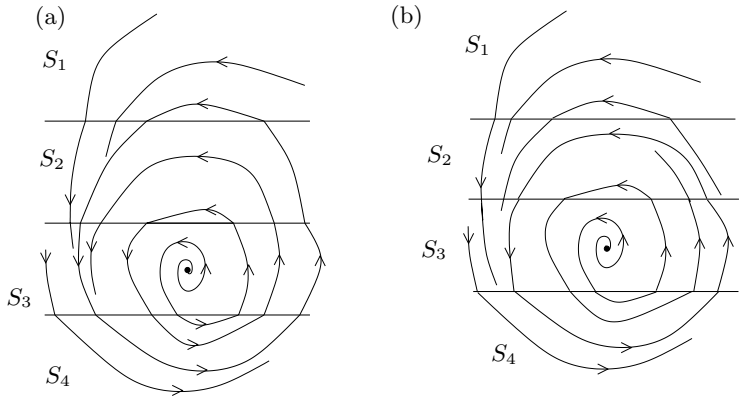

Fig. 2.24. Two phase potraits that are topological equivalent but not piecewise topological equivalent according to Definition 2.30. Note that the portrait in each separate region S_i, $i = 1, \dots, 4$ is topological equivalent between (a) and (b); yet in (a) there is a limit cycle that does not enter all four phase space regions, whereas in (b) the corresponding limit cycle does not visit region S_1. If a parameter is varied between these two cases, a DIB must occur, in this case, a grazing bifurcation of the limit cycle with the boundary Σ_{12}.

To motivate the second part of this definition, we want to call the two phase potraits illustrated in Fig. 2.24 non-equivalent, because in panel (a) there is a limit cycle that visits all four phase space regions, whereas in (b) the limit cycle visits only three of them. To see that this example fails the definition of equivalence, note that to transform from one phase portrait to another the limit cycle must be 'pulled through' the boundary Σ_{12}. Such a transformation cannot be achieved in a continuous way. In other words, the limit cycle and Σ_{12} are not in the same *general position* with respect to each other. This then leads us to our topological definition of a *discontinuity-induced bifurcation* (DIB) for parameterized piecewise-smooth dynamical systems. For example, we shall want to say that a discontinuity-induced bifurcation must occur if

we continuously vary parameters between those used to obtain the two phase potraits in Fig. 2.24.

The definition of DIB proceeds as for the definition of smooth bifurcations. We start by saying what we mean by structural stability:

Definition 2.31. *A piecewise-smooth system is* **piecewise-structurally stable** *if there is an $\varepsilon > 0$ such that all C^1 perturbations of maximum size ε of the vector field (map) f, that leave the number and degree of smoothness properties of each of the boundaries Σ_{ij} unchanged, lead to piecewise-topological equivalent phase potraits.*

Definition 2.32. *A* **discontinuity-induced bifurcation** *(DIB) occurs at a parameter value at which a piecewise-smooth system is not piecewise-structurally stable. That is, there exists an arbitrarily small perturbation that leads to a system that is not piecewise-topological equivalent.*

Remarks

1. Note that we have been somewhat imprecise about what kind of perturbations are allowed in Definitions 2.31 and 2.32. One wants only to consider perturbed systems for which the partitioning of phase space into regions S_i remains topologically the same and that the degree of smoothness across each boundary does not change. We also want that the resets R_{ij} map boundaries Σ_{ij} to the equivalent parts of phase space. In fact, it remains an open problem to show that Definitions 2.30 and 2.32 are well defined mathematically. Strictly speaking, we need to define a topological space for each class of piecewise-smooth system in order to define topological equivalence correctly. The rigorous theory of DIBs is still in its infancy, and we shall not pursue this further here. Rather we shall treat Definition 2.32 as a working definition.
2. The concepts of *codimension* and *unfolding* can also be constructed, as in Definition 2.16 for bifurcations in smooth systems, but here one has to be even more careful to state what kinds of perturbation are allowed. Again we adopt a working definition of codimension that it is the 'degree of unlikeliness' of the discontinuity-induced bifurcation. That is, how many parameters would one expect to have to vary in order to correctly unfold the bifurcation?
3. Under Definition 2.32 classical bifurcations are also DIBs. However, our main focus in this book is the particular class of discontinuity-induced bifurcations that are caused by something structurally unstable happening with respect to a discontinuity set Σ_{ij}. Bifurcations that have nothing to do with discontinuity sets we shall refer to as *smooth bifurcations*. Most of the rest of this book will be about cataloging the various non-smooth transitions (particularly those of codimension-one) that can occur in piecewise-smooth systems. We shall also provide unfoldings of the ensuing dynamics and ways of calculating these unfoldings in examples. Moreover we shall seek to show how these DIBs explain the observed dynamics.

4. In the special case of Filippov systems in $\mathbb{R}^3$ there is now a rigorous structural stability theory; see the work by Filippov [100], Teixera [248], Simic & Johansson [239] and references therein.

2.4.3 Types of discontinuity-induced bifurcations

The main aim of rest of this book is devoted to a classification and analysis of the most commonly occurring types of DIBs. As we shall see, these lie at the heart of explaining what was observed in the case study examples introduced in Chapter 1. Let us list some of the most commonly occurring types of codimension-one DIBs (see Fig. 2.25):

Border collisions of maps. These are conceptually the simplest kind of DIB and occur when, at a critical parameter value, a fixed point of a piecewise-smooth map lies precisely on a discontinuity boundary Σ. For maps with singularity of order one (i.e., locally piecewise-linear continuous), there is now a mature theory for describing the bifurcation that may result upon varying a parameter through such an event. Remarkably, the unfolding may be quite complex. Even in one dimension, we saw in case study VIII that a period-1 attractor can jump to a period-n attractor for any arbitrary n, or to robust chaos without any periodic windows. In one and two dimensions, more or less everything is known. But in general n-dimensional maps, bifurcation information on only the simplest kinds of periodic points is known. This material is presented in Chapter 3. Chapter 4 then goes on to study border collision bifurcations in maps with other degrees of singularity, including the discontinuous and square-root cases from case studies VI and VII.

Boundary equilibrium bifurcations. The simplest kind of DIB for flows occurs when an equilibrium point lies precisely on a discontinuity boundary Σ. In Filippov systems and hybrid systems with sticking regions, there is also the possibility of *pseudo-equilibria*, which are equilibria of the sliding or sticking flow but are not equilibria of any of the vector fields of the original system. There are thus possibilities where the equilibrium lies precisely on the boundary between a sliding or sticking region and a pseudo-equilibrium turns into a regular equilibrium (either under direct parameter variation or in a fold-like transition where both exist for the same sign of the perturbing parameter). There is also the possibility that a limit cycle may be spawned under parameter perturbation of the boundary equilibrium, in a Hopf-like transition. This material is treated in Chapter 5.

Grazing bifurcations of limit cycles. One of the most commonly found DIBs in applications is caused by a limit cycle of a flow becoming tangent to (i.e., grazing) with a discontinuity boundary. One might naively think that this can be completely understood (upon taking an appropriate Poincaré section that contains the grazing point) as a border collision. However, as

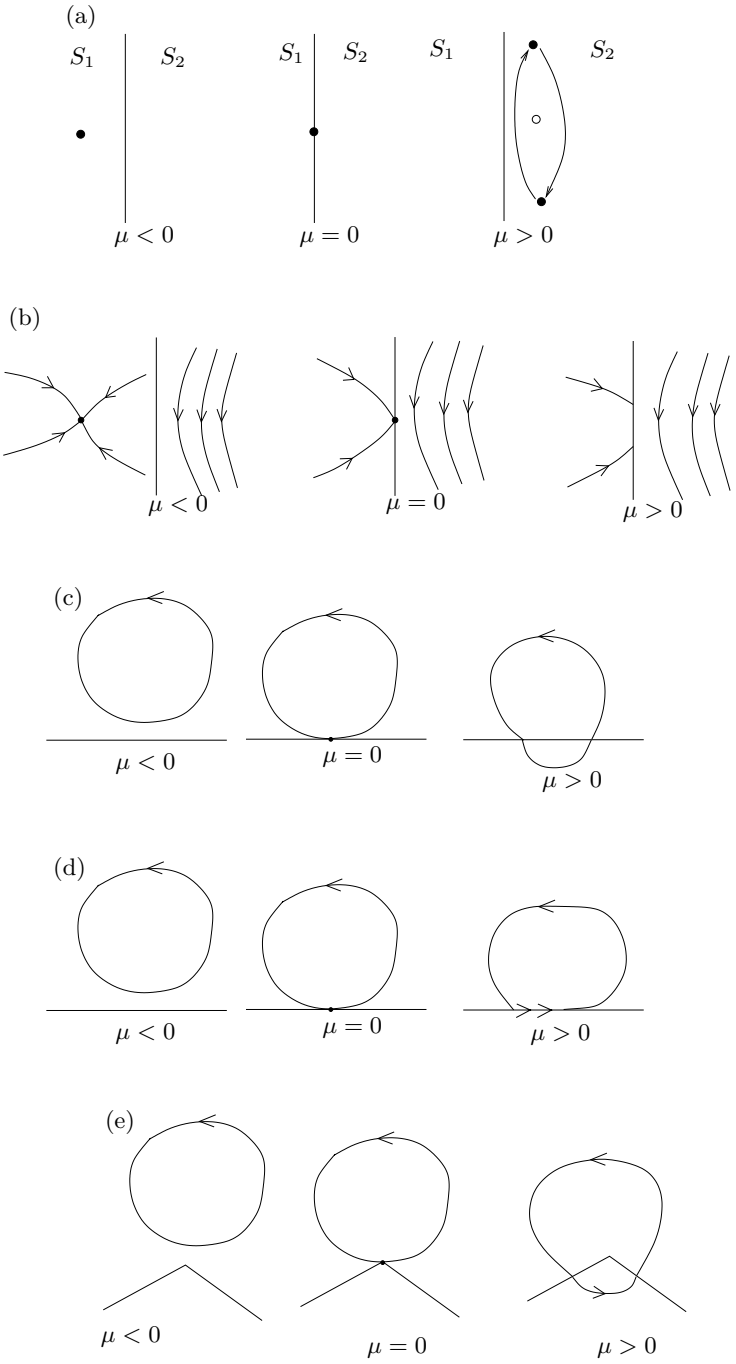

Fig. 2.25. Examples of DIBs: (a) a border collision in a map; (b) a boundary equilibrium bifurcation; (c) a grazing bifurcation of a limit cycle; (d) a sliding bifurcation in a Filippov system; (e) a boundary intersection crossing.

we shall see in Chapter 6 for hybrid systems and Chapter 7 for piecewise-smooth ODEs this is not necessarily the case. Instead one has to analyze carefully what happens to the flow in the neighborhood of the grazing point. In fact, one can derive an associated map (the, so-called, discontinuity map). But, the link between the singularity of the map and the degree of smoothness of the flow is a subtle one that also depends on whether the flow is uniformly discontinuous at the grazing point. This analysis explains what is observed at the grazing bifurcations in the impact and bi-linear oscillators, case studies I and II.

Sliding and sticking bifurcations. There are several ways that an invariant set such as a limit cycle can do something structurally unstable with respect to the boundary of a sliding region in a Filippov system. Chapter 8 is devoted to a careful unfolding of each of these. The Poincaré maps so derived have the property of typically being noninvertible in at least one region of phase space, owing to the loss of information backward in time inherent in sliding motion. This analysis helps to explain the dynamics observed in the relay control and dry friction examples described in case studies III and IV. In addition, in impacting systems, sticking regions can be approached by infinite *chattering* sequences of impacts, which we have seen already in case study I. Further details of such events will be given in Chapter 6 in the context of the single degree-of-freedom impact oscillator.

Boundary intersection crossing/corner collision. Another possibility for a codimension-one event in a flow is where an invariant set (e.g., a limit cycle) passes through the $(n-2)$-dimensional set formed by the intersection of two different discontinuity manifolds Σ_1 and Σ_2. In Chapter 7 we shall consider such intersection crossing in Filippov systems in the case where there is no sliding. We also consider there the special case where the jumps in vector field across Σ_1 and Σ_2 are such that their intersection can be considered as a 'corner' in a single discontinuity surface. This can explain the dynamics observed in the DC–DC converter, case study V.

Some possible global bifurcations. One example, which we shall mention in Chapter 5, involves a connection between the stable and the unstable manifolds of *pseudo-equilibria*, which are equilibria of a sliding flow but not of the individual flows either side of a discontinuity boundary.

Chapter 9 briefly treats extensions to the theory of DIBs, which are in each case motivated by a further case study example of practical significance, for which a detailed treatment is beyond the scope of the book. Topics include parameter and noise sensitivity; bifurcations that involve invariant tori grazing with a discontinuity surface; the similarity between grazing in piecewise-smooth flows and hybrid systems in the limit of large discontinuities; and codimension-two bifurcations.

2.5 Discontinuity mappings

The analysis of discontinuity-induced bifurcation in maps is relatively straightforward; one merely has to consider the fate of iterates that land either side of the discontinuity. DIBs in piecewise-smooth flows or hybrid systems are far harder to analyze, because one must establish the fate of topologically distinct trajectories close to the structurally unstable event that determines the bifurcation. In this section we introduce a key analytical tool that enables the study of DIBs involving limit cycles and other invariant sets that are more complex than mere equilibria. The concept is that of a *discontinuity map* (DM), a term first introduced by Nordmark [197]. This is a synthesized Poincaré mapthat is defined *locally* near the point at which a trajectory interacts with a discontinuity boundary. When composed with a global Poincaré map(for example around the limit cycle) ignoring the presence of the discontinuity boundary, one can then derive a (typically non-smooth) map whose orbits completely describe the dynamics in question.

To illustrate why discontinuity maps are both necessary and useful, consider the piecewise-smooth flow illustrated in Fig. 2.26(a),(b), for which there is a Poincaré surface Π lying in one of the regions S_i, which is intersected transversally at the point x_p by a periodic orbit $p(t)$ of period T.

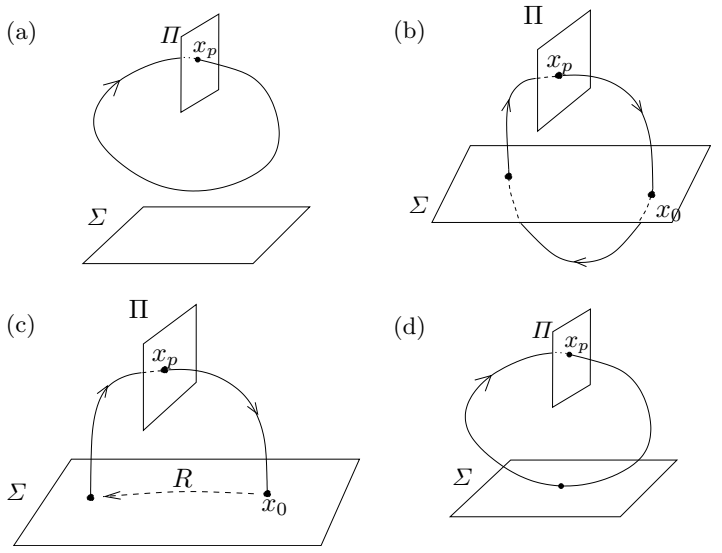

Fig. 2.26. (a) Simple periodic orbit $p(t)$ in piecewise smooth ODE that does not intersect any discontinuity surfaces. (b) Simple periodic orbit that intersects a single surface twice. (c) Equivalent to (b) but for an impacting hybrid system. (d) A grazing periodic orbit.

For points $\widehat{x} \in \Pi$ close to x_p, we may define a Poincaré map $P : \Pi \to \Pi$. It is natural to ask what form P takes when $\|x - x_p\|$ is small. The answer to this question takes three forms, and depends crucially upon the nature of the orbit $p(t)$.

If $p(t)$ lies wholly inside S_i, as in Fig. 2.26(a) then nearby orbits will also lie inside S_i. In this case the time-T map starting from x will be the smooth flow map $P(x) = \Phi_i(x, t)$, which has a well-defined Taylor series,

$$P(x) = N(x - x_p) + O\left(|x - x_p\|^2\right), \tag{2.67}$$

where $N = \Phi_{i,x}(x_p, T)$ is the Jacobian derivative with respect to x of the flow Φ_i around the periodic orbit, evaluated at $x = x_p$. More interesting things happen if the periodic orbit $p(t)$ intersects discontinuity surfaces Σ_{ij}.

Consider next the case illustrated in Fig. 2.26(b), where $p(t)$ has two *transverse* intersections with a discontinuity set Σ. In this case it is tempting to write that the linearization of the Poincaré maptakes the form $P(x) = N_1 N_2 N_3 (x - x_p)$, where N_1, N_2 and N_3 are linearizations of the flows Φ_1, Φ_2 and Φ_1, respectively, for the appropriate times for the trajectory starting at x_p to, respectively, reach Σ for the first time, to pass between the first and second intersections of Σ, and to pass from Σ back to Π. However, this is not the case because, as we shall see in Sec. 2.5.2, each time Σ is crossed transversally, one must apply a correction to the Poincaré map. This correction is necessary because the time taken for trajectories at points x close to x_p to reach the discontinuity boundary Σ will in general vary, and so a small error will be made in assuming that the linearization required is that of Φ_1 for a constant time. The correction to this error is the discontinuity map in this case. The effect of the DM on the matrix N_1 is to multiply it by a so-called *saltation matrix* [2, 194, 173] whose derivation we give below. A similar correction must be applied to the matrix N_2. Not introducing these corrections will in general result in wrong conclusions being made about the Floquet multipliers of the periodic orbit $p(t)$. Note in this case, provided the form of the jump in the vector fields upon crossing Σ is described by a smooth function, then the discontinuity mapping and the associated global Poincaré maparound $p(t)$ will both be smooth. Similar considerations apply to impacting hybrid systems where a periodic orbit $p(t)$ has a single impact with a discontinuity surface as in Fig. 2.26(c).

Now consider for a moment the special case where the velocity normal to Σ is zero, so that the periodic orbit *grazes* the discontinuity surface, as in Fig. 2.26(d). Note that the trajectories from some initial conditions $x \in \Pi$ near x_p do not intersect Σ at all, whereas others intersect Σ with a low normal velocity. The discontinuity mapping in this case is the identity for orbits that do not cross Σ, but is defined as the local correction that must be applied to initial conditions that *do* cross Σ, so that a Poincaré mapcan be applied as if Σ were not there. As we shall motivate briefly in Sec. 2.5.3 below, the effect of applying the DM to the map in (2.67) in this case is to introduce additional terms proportional to fractional powers of $\|x - x_p\|$, such as $\|x - x_p\|^{1/2}$ or

$\|x - x_p\|^{3/2}$. An analysis of the behavior of maps with fractional powers will be given in Chapter 4. Detailed derivations of DMs close to different kinds of DIBs, along with analyzing their dynamical consequences, form the main subject Chapters 6, 7 and 8.

In the case that trajectories intersect discontinuity boundaries transversally, then typically one still has to compute a discontinuity mapping in order to derive a globally correct Poincaré map. This is because even though the trajectory itself may be continuous (or in the case of a hybrid system, the trajectory's evolution would be defined by a continuous reset map), there is a correction that must be to the first and higher derivatives of the flow. This correction arises because the discontinuity boundary acts like a new Poincaré section that is distinct from the fixed time-t section that is implicitly defined flow.

2.5.1 Transversal intersections; a motivating calculation

Before deriving the general form of the *transverse discontinuity mapping* for an arbitrary piecewise-smooth or hybrid system, let us start with the motivating case of a simple impacting hybrid system of the form (2.35) and (2.36). Here we assume a smooth reset map R applies whenever the smooth flow Φ, governed by vector field F, impacts the discontinuity surface $\Sigma := \{x : H(x) = 0\}$ transversally; see Fig. 2.27. We shall analyze the dynamics of a trajectory with initial condition $\widehat{x}$ that is close to a reference trajectory x_p that impacts $\Sigma := \{x : H(x) = 0\}$ at a point x_*. It is perhaps most useful to think of x_p as belonging to a periodic orbit $p(t)$, for which x_* is the unique point of impact; although the analysis that follows shall be entirely local to a neighborhood of x_*. Let us define t_1 to be the time for which $\Phi(x_p, t_1) = x_*$ and let x_0 be the point reached by flowing for the same time from initial condition $\widehat{x}$, so that $\Phi(\widehat{x}, t_1) = x_0$. Note that, in general, x_0 will not lie in Σ. Instead, we must continue the flow for a small additional time δ (which may be positive or negative) until the trajectory intersects Σ. From this intersection point, the map R is applied to reach the point x_3 in Fig. 2.27. Now, the discontinuity map Q is defined to be the mapping that takes x_0 to x_4, which is the point obtained by flowing from x_3 through a time $-\delta$. That is,

$$Q(x_0) = \Phi(x_3, -\delta) = \Phi(R(\Phi(x_0, \delta)), -\delta).$$

Thus, Q maps x_0 to the appropriate point on the trajectory of the true hybrid flow which, without resetting the time variable, can be evolved forward under Φ as if the impact had occurred at time t_1. In the case that $x_0 \in \Sigma$, then note that by definition $\delta = 0$ and Q reduces to the reset map R. However, for general points x_0 close to x_*, Q contains an additional correction. We shall now proceed to derive an expression for the leading-order correction.

For a general flow described by the differential equation $\dot{x} = F(x)$, the solution for small subsequent times δ starting from the point x_0 can be expressed as a Taylor series in δ:

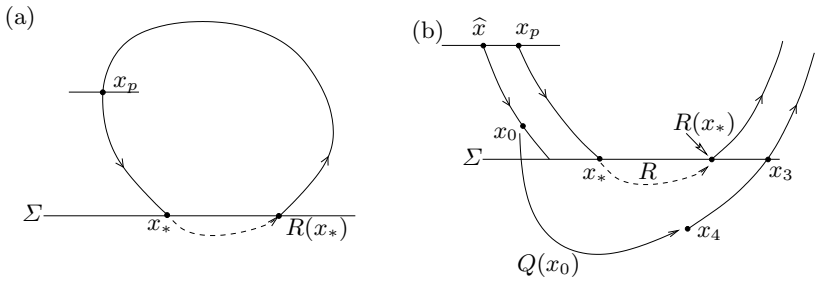

Fig. 2.27. (a) An impacting periodic orbit. (b) A blow-up near x_* defining the transverse discontinuity mapping $Q(x)$.

$$x(t) = \Phi(x_0, \delta) = x_0 + \delta F(x_0) + O(\delta^2).$$

Setting $x_0 = x_* + \Delta x$, we obtain

$$x(t) = x_* + \Delta x + \delta F(x_*) + O(\delta^2, \delta\Delta x, (\Delta x)^2).$$

We wish to find the time δ for which $H(x(\delta)) = 0$. Thus we require

$$H\left(x_* + \Delta x + \delta F(x_*) + O(2)\right) = 0. \tag{2.68}$$

where $O(2)$ refers to general quadratic terms in the small variables δ and Δx. Now, because $H(x_*) = 0$, we find for x close to x_*

$$H = H_x(x_*)(x - x_*) + O(\|x - x_*\|^2).$$

Hence, from (2.68) we seek a solution δ to the equation

$$0 = H_x(x*)\left[\Delta x + \delta F(x_*)\right] + O(2)$$

Thus, we find

$$\delta = -\frac{H_x(x_*)\Delta x}{H_x(x_*)F(x_*)} + O(2). \tag{2.69}$$

Note that this expression is only valid provided $H_x(x_*)F(x_*) \neq 0$, which is precisely the condition that the flow crosses Σ *transversally*, i.e., with non-zero velocity. Applying the reset map to the point $\Phi(x_0, \delta)$ gives for x_3:

$$x_3 = R[x_* + \Delta x + \delta F(x_*)] + O(2).$$

To obtain the discontinuity map we must find an expression for x_4 in the form

$$\begin{aligned} x_4 &= \Phi(x_3, -\delta) \\ &= x_3 - \delta F(x_3) + O(2) \\ &= R[x_* + \Delta x + \delta F(x_*)] - \delta F\left(R[x_* + \Delta x + \delta F(x_*)]\right) + O(2). \end{aligned}$$

Now, both R and F can be expanded as Taylor series about x_*. Hence, we obtain

$$x_4 = R(x_*) + R_x(x_*)[\Delta x + \delta F(x_*)] - \delta F(R_x(x_*)) + O(2).$$

Using the expression (2.69) for δ, we finally obtain

$$x_4 = R(x_*) + \frac{R_x(x^*) + [F(R(x_*)) - R_x(x_*)F(x_*)]H_x(x_*)}{H_x(x_*)F(x_*)}\Delta x + O(2).$$

Recalling that $\Delta x := x_0 - x^*$, note that $R(x^*) + R_x(x^*)\Delta x + O(2)$ is just the first the first two terms in the Taylor expansion of $R(x_0)$. Hence, the transverse discontinuity mapping is given, to leading order, by

$$x_0 \to Q(x_0) = R(x_0) + \frac{[F(R(x_*)) - R_x(x_*)F(x_*)]H_x(x_*)}{H_x(x_*)F(x_*)}(x_0 - x_*). \quad (2.70)$$

The second term in (2.70) is the leading-order correction to the reset map $R(x_0)$; note that this term is linear in $(x_0 - x_*)$. Hence, failure to apply this mapping when computing periodic orbits with impacts will in general lead to incorrect linearizations (Monodromy matrices), hence incorrect Floquet multipliers and (potentially) incorrect conclusions about stability of the periodic orbit.

2.5.2 Transversal intersections; the general case

Consider now a general hybrid system (2.32), (2.33) in $\mathbb{R}^n$, which we assume to have two phase space regions S_1 and S_2 as illustrated in Fig. 2.28, with corresponding flows Φ_1 and Φ_2, and a single reset map R applying on the boundary Σ between the two regions. Note that this covers both the case of a piecewise-smooth flow (2.23) and an impacting hybrid system (as in the previous calculation). In the case of a piecewise-smooth flow, the reset map R is the identity mapping. For the impacting hybrid system, R maps $\Sigma \to \Sigma$, and the flow Φ_1 applies after the impact, so that the flow Φ_2 becomes identically Φ_1 in what follows.

Suppose that a periodic orbit $p(t)$ crosses the discontinuity set Σ transversally at the two points $x = x_*$ and x_{**} as illustrated in Fig. 2.28. The key observation is that all nearby trajectories must then cross Σ transversally. Then, since R, Φ_1 and Φ_2 are smooth, the Poincaré map associated with this periodic orbit is smooth and has non-singular Jacobian. To compute this Jacobian, and indeed the entire Poincaré map, consider the flow map for the specific sequence of events that ensue from an initial condition x close to x_p in a Poincaré section Π.

Let us choose an origin of time such that the periodic orbit intersects the Poincaré section Π at $x_p \in S_1$ when $t = 0$ and intersects Σ at the two times $t_2 > t_1 > 0$. Trajectories close to the point x_* and the time t_1 are depicted in Fig. 2.28(b).

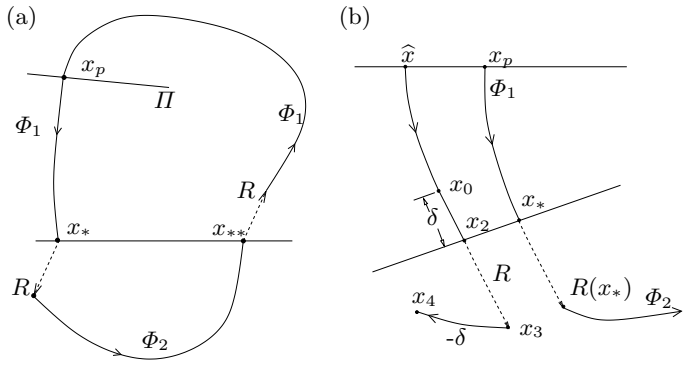

Fig. 2.28. (a) Defining the event sequence for a simple periodic orbit that generalizes the two cases in Fig. 2.26. (b) Construction of the transverse discontinuity mapping $Q : x_0 \mapsto x_4$.

Taking a nearby initial condition x to x_p and evolving the flow forward leads to a trajectory that intersects Σ at the point x_2 close to x_*, at time $t_1 + \delta$. If, in contrast, we evolve the flow from x for a fixed time t_1, we reach the point $x_0 = \Phi_1(x, t_1)$ in the figure. Applying the map R and then the flow Φ_2 to the point x_0 for $t > t_1$ gives an error as we have applied R at x_0 and $t = t_1$ rather than at x_2 and at $t = t_1 + \delta$. To correct this we can find the point x_4 such that the action of Φ_2 on the point x_4 for future times $t > t_1$ coincides with the action of Φ_2 on the point $x_3 = R(x_2)$ for $t > t_1 + \delta$. The correction $x_4 = Q(x_0)$ is indicated in the figure and is the *discontinuity mapping* in this case. This correction is applied to the point x_0 and can be defined theoretically by the expression

$$Q(x_0) = \Phi_2(R(\Phi_1(x_0, \delta)), -\delta) = \Phi_2(x_3, -\delta). \tag{2.71}$$

The points x_0, x_2, x_3 and x_4 are all indicated in Fig. 2.28(b). Note that the total elapsed time of the flow combination described by the discontinuity map is $\delta - \delta = 0$.

A similar map can be applied to the subsequent intersection with Σ at the point x_{**}. Then, the time-T map for the evolution of the overall piecewise-smooth flow around $p(t)$ becomes

$$P(x, T) = \Phi_1[Q(\Phi_2[Q(\Phi_1[x_p, t_1]), t_2 - t_1]), T - t_2],$$

which has Jacobian derivative

$$P_x(x, T) = \Phi_{1,x}[R(x_{**}), T - t^0]Q_x(x_{**})\Phi_{2,x}[R(x_*), t^0 - t_0]Q_x(x_*), \Phi_{1,x}(x_p, t_0) \tag{2.72}$$

where Q_x is the linearization of (2.71).

Definition 2.33. *The* **transverse discontinuity map** Q *for the transverse crossing of a discontinuity set* Σ_{ij} *in a piecewise-smooth flow (or hybrid system) is the extra mapping that the flow maps* Φ_i *and* Φ_j *must be composed with in order to get a description of the piecewise-smooth (hybrid) flow. Thus, if* Σ *is crossed in the sense of passing from region* S_i *to* S_j*, the correct flow map is* $\Phi_2 \circ Q \circ \Phi_1$*. The Jacobian derivative* Q_x *of* Q *is called the* **saltation matrix**.

We shall now extend the earlier calculation to derive an explicit expression for the discontinuity mapping Q, and its derivative, the saltation matrix Q_x. In order to do so, suppose that the discontinuity set can be written locally as

$$\Sigma = \{x \in \mathbb{R}^n : H(x) = 0\}$$

for some smooth function H. Consider again the local piece of the trajectory in Fig. 2.27 with initial condition x in a neighborhood of x_p. Evolving through a time t_1 we reach the point $x_0 = \Phi_1(x, t_1)$, which is in a small neighborhood of the point $x_* = \Phi_1(x_p, t_1)$. We suppose that $x_0 = x_* + \Delta x$, where $\|\Delta x\|$ is small and develop a Taylor series for $\Phi_1(x_0, \delta)$, for small times δ.

For a flow described by the differential equation $\dot{x} = F_1(x)$, the solution for subsequent times δ starting from the point x_0 is given by

$$\Phi(x_0, \delta) = x_0 + \delta F_1(x_0) + \frac{\delta^2}{2} F_{1,x}(x_0) F_1(x_0) + O(\delta^3).$$

If we now set $x_0 = x_* + \Delta x$ this expression takes the form

$$x(t) = x_* + \Delta x + \delta F_1(x_*) + \delta \Delta x F_{1,x}(x_*) + \frac{\delta^2}{2} + F_{1,x}(x_0) F_1(x_0) + O(3). \quad (2.73)$$

Here $O(3)$ refers to cubic terms in δ and Δx. The transversality of the intersection of $p(t)$ with Σ allows us to assume that these are of the same order.

The first step to computing $Q(x_0)$ is to find the time δ and the point x_2 at which $H(x_2) = H(\Phi_1(x_0, \delta)) = 0$. Thus

$$H\left[x_* + \Delta x + \delta F_1(x_*) + \delta \Delta x F_{1,x}(x_*) + F_{1,x}(x_*) F_1(x_*) \delta^2/2 + O(3)\right] = 0. \quad (2.74)$$

Now, as $H(x_*) = 0$, the function H can also be expanded in x about x_* as

$$H(x) = H_x(x_*)(x - x_*) + \frac{1}{2}(x - x_*)^T H_{xx}(x_*)(x - x_*) + O(3).$$

So (2.74) can also be expressed as a Taylor series and solved term by term for δ, under the assumption that the leading-order term

$$H_x(x_*) F_1(x_*) \neq 0. \quad (2.75)$$

As before, this is precisely the condition that $p(t)$ crosses Σ *transversally.* Specifically we obtain

$$\delta = -\frac{H_x(x_*)\Delta x}{H_x(x_*)F_1(x_*)} + O(2), \qquad x_2 = x_* + \Delta x + \delta F_1(x_*) + O(2),$$

The quadratic and all higher terms in these expressions can also be evaluated if higher-order expressions for the discontinuity mapping are required. In fact, the assumption (2.75) guarantees that the discontinuity map Q is an analytic function provided F_1, F_2 and R are also analytic.

According to (2.71), we now compute Q by applying the flow Φ_2 to the point

$$x_3 := R(x_2) = R\left[x_* + \Delta x + \delta F_1(x_*)\right] + O(2).$$

for a time $-\delta$. Now, Φ_2 can be expanded about the point $R(x_*)$ in the same way as Φ_1 was expanded about x_*; see (2.73). This gives

$$\begin{aligned} Q(x_0) &= x_4 = \Phi_2(x_3, -\delta) \\ &= R(x_2) - F_2(R(x_2))\delta + O(2) \\ &= R(x_0 + \delta F_1(x_*)) - F_2(R(x_0 + \delta F_1(x_*)))\delta + O(2). \end{aligned}$$

Furthermore, we will assume that the map R can be expanded about the point x_*, so that

$$R(x_0) = R(x_*) + R_x(x_*)\Delta x + \frac{1}{2}\Delta x^T R_{xx}(x_*)\Delta x + O(3).$$

Using this expression we have

$$\begin{aligned} Q(x_0) &= R(x_*) + R_x(x_*)\Delta x + R_x(x_*)F_1(x_*)\delta\Delta x - F_2(R(x_*))\delta\Delta x + O(2) \\ &= R(x_*) + \left[R_x + \frac{H_x(x_*)}{H_x(x_*)F_1(x_*)}[F_2(R(x_*)) - R_x(x_*)F_1(x_*)]\right](x_0 - x_*) \\ &\quad + O(\|x_0 - x_*\|^2). \end{aligned} \tag{2.76}$$

Thus, the saltation matrix Q_x in this general case is given by

$$Q_x(x_*) = R_x(x_*) + \frac{[F_2(R(x_*)) - R_x(x_*)F_1(x_*)]H_x(x_*)}{H_x(x_*)F_1(x_*)}.$$

We now consider examples where we can calculate the saltation matrix explicitly.

Example 2.12 (A two-zone Filippov system without sliding). For Filippov systems in which $R(x) = x$ and $F_1 \neq F_2$ the saltation matrix is given by the expression

$$Q_x = I + \frac{(F_2 - F_1)H_x}{H_x F_1}, \tag{2.77}$$

where I is the identity matrix. This expression was first derived in [2].

Example 2.13 (Impacting systems). For impacting systems with a single impact boundary written in the form (2.35), (2.36). the vector field F_2 should be identified with F_1, since the R maps Σ^- to Σ^+. Upon letting $F_1 = F_2 := F$, we find that

$$Q_x(x_*) = R_x(x_*) + \frac{[F(R(x_*)) - R_x(x_*)F(x_*)]H_x(x_*)}{H_x(x_*)F(x_*)}, \tag{2.78}$$

which is precisely the linearization of (2.70) derived earlier.

As a specific application, consider the one-dimensional impact type hybrid system considered in case study I, in which $x = (x_1, x_2, x_3)$, $H(x) = x_1 - \sigma$, $R(x) = (x_1, -rx_2, x_3)$ and $F(x) = (x_2, a, 1)$, with $a = \cos(\omega t)) - x_1 - 2\zeta x_2$ being the acceleration. (Note that the subscripts here refer to vector indices rather than to the points in the Fig. 2.27.) We therefore have

$$R_x = \begin{pmatrix} 1 & 0 & 0 \\ 0 & -r & 0 \\ 0 & 0 & 1 \end{pmatrix}, \quad H_x = (1, 0, 0).$$

If we set $v = H_x(x_*)F(x_*)$ to be the normal velocity immediately before impact and a^- and a^+ to be the normal accelerations immediately before and immediately after the impact, we obtain

$$\begin{aligned} Q_x &= \begin{pmatrix} 1 & 0 & 0 \\ 0 & -r & 0 \\ 0 & 0 & 1 \end{pmatrix} + \frac{1}{v}\left[\begin{pmatrix} -rv \\ a^+ \\ 1 \end{pmatrix} - \begin{pmatrix} 1 & 0 & 0 \\ 0 & -r & 0 \\ 0 & 0 & 1 \end{pmatrix}\begin{pmatrix} v \\ a^- \\ 1 \end{pmatrix}\right](1, 0, 0) \\ &= \begin{pmatrix} -r & 0 & 0 \\ \frac{a^+ + ra^-}{v} & -r & 0 \\ 0 & 0 & 1 \end{pmatrix} = \begin{pmatrix} -r & 0 & 0 \\ \frac{1+r}{x_2}(\cos\omega t - \sigma) & -r & 0 \\ 0 & 0 & 1 \end{pmatrix}, \end{aligned} \tag{2.79}$$

which is a result first derived by Fredriksson and Nordmark [107].

Example 2.14 (Onset of sliding in Filippov systems). Saltation matrices also apply for trajectories of Filippov systems that undergo a transition into sliding, as depicted in Fig. 2.29. Proceeding as above it is straightforward to derive that the saltation matrix for this case is

$$Q_x = I + \frac{(F_{12} - F_1)H_x}{H_x F_1},$$

where F_{12} is the sliding flow defined by (2.80).

2.5.3 Non-transversal (grazing) intersections

The above discontinuity mapping (2.76) was derived under the transversality condition (2.75). So-called *grazing* occurs when a trajectory becomes tangent

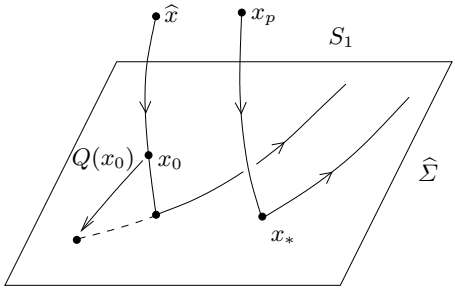

Fig. 2.29. Defining the saltation matrix for the onset of sliding.

to a discontinuity surface Σ. This occurs precisely when (2.75) is violated; that is, when $v := H_x(x_*)F_1(x_*) = 0$. Notice, from the expression (2.76) that the saltation matrix contains terms which are proportional to $1/v$ as $v \to 0$. Specifically, the coefficient of $1/v$ is $F_2 - F_1$, which would be zero in the case of flow with degree of smoothness two or higher. However, evaluation of subsequent terms in the Taylor expansion of the discontinuity map show that the factor $1/v$ enters at all orders, such that discontinuity with smoothness degree $n-2$ implies a singularity (proportional to $1/v$) of the nth derivative of the discontinuity map. Thus, the map is no longer analytic in the case of a grazing impact. In fact, detailed calculations which will be given in Chapters 6, 7 and 8 show that we should expect terms like $\sqrt{\Delta x}$ to occur in the expressions for the resulting discontinuity maps in this case. However, first we have to explain what we mean by a discontinuity map in the case of a grazing impact.

We illustrate the situation close to a grazing for an impacting hybrid system in Fig. 2.30. In this figure, which is analogous to Fig. 2.27, we show a distinguished trajectory locally lying entirely S_1. This trajectory we assume to graze with the discontinuity boundary Σ at the point x_* at time t_0.

To construct the discontinuity mapping, we need to know the fate of two different types of trajectory with initial conditions close to x_*. Some trajectories do not cross Σ locally; for these, the discontinuity mapping is the identity. In contrast, the discontinuity mapping will be non-trivial for the trajectory illustrated in Fig. 2.30 that passes through the point x_0 close to Σ at time t_1, hits Σ at the point x_2 at time $t_0 + \delta$, is mapped to the point x_3 by the map $\Phi_2(R(x_2), t_2 - t_1)$ and continues in S_1 from this point. Note that we allow here for both the impacting hybrid system case, in which Φ_2 is the identity, or the piecewise-smooth flow case, where R is in the identity. In the latter case, $t_2 - t_1$ is the time of flight of the trajectory until its second impact with Σ.

We shall describe two different ways of defining the non-trivial part of the discontinuity map. These are constructed either, like the DM for transversal trajectories defined above, such that the total elapsed time is zero—a so-called *zero-time discontinuity mapping (ZDM)*—or are defined with respect to a local *Poincaré* section—a *Poincaré-section discontinuity mapping (PDM).*

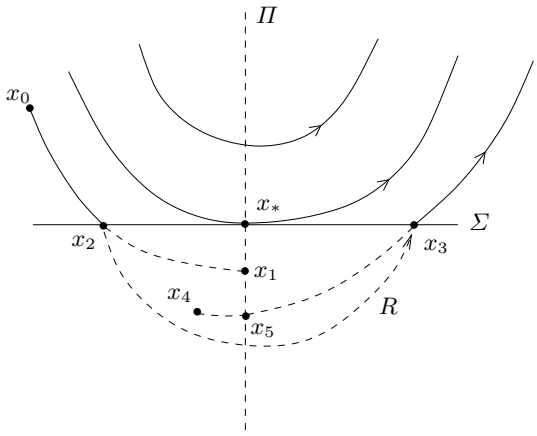

Fig. 2.30. A local illustration of the ZDM and PDM close to a grazing in an impacting hybrid system. In this figure the solid line represents the actual flow of the hybrid system, and the dashed line the extended flow. The ZDM is the map $x_0 \mapsto x_4$ and the PDM is the map $x_1 \to x_5$.

Our treatment is inspired by the analysis of n-dimensional impacting systems by [106], which extends earlier results in [236, 264, 197, 142].

To explain the difference between the ZDM and the PDM, consider in more detail the trajectory in Fig. 6.7 that passes through x_0. It intersects the Σ at x_2 and is mapped to x_3, where it subsequently evolves to the point x_6. By extending the smooth flow field $F_1(x)$ defined in the region $H(x) > 0$ (so that it lies above Σ in S_1) to the region $H(x) < 0$ (so that it now lies below Σ), we may continue the trajectory forward from x_2 under the action of the flow map Φ_1, or equally backward from x_3. As the point x_0 is close to x_g, then the smooth trajectory carried forward from x_2 under the action of Φ_1 will intersect the Poincaré surface

$$\Pi_N = \{x : v = H_x(x)F_1(x) = 0\}$$

at a point x_1 close to $x_g = 0$. Similarly, the backward continuation of the flow from x_3 will intersect the set Π_N at the point x_5. The mapping which takes x_1 to x_5 is the PDM.

Definition 2.34. *The* **Poincaré-section discontinuity mapping (PDM)** *near a grazing orbit is the discontinuity mapping defined on a suitable surface Π_N transverse to the flow, which contains the grazing set and intersects Σ transversally, that takes initial conditions on Π_N back to themselves. There is no requirement that this map take zero time.*

The same trajectory starting from x_3 can also be continued backward under the action of Φ_1 for a time $-\delta$ so that it passes through the point x_4 at the time t_0. We then define the ZDM as the map from x_0 to x_4.

Definition 2.35. *The* **zero-time discontinuity mapping (ZDM)** *near a grazing orbit is the discontinuity mapping in a neighborhood of the grazing point x_0 that takes zero time. That is, when this map is composed with the flow map of the non-impacting system in order to define a trajectory of the full system, the time taken is the same as for the flow map alone.*

In order to analyze *grazing bifurcations* of periodic orbits, we suppose that the trajectory passing through x_* is part of a limit cycle $p(t)$. Then, in order to unfold the dynamics, we need to combine a grazing discontinuity mapping (PDM or ZDM) with a Poincaré map defined around the limit cycle ignoring the grazing point. For example, zero time condition allows the ZDM to be incorporated in a natural way into the calculation of a fixed time-T Poincaré map P_S, sometimes called a *stroboscopic map*. For instance, for a grazing periodic orbit that is contained entirely within region S_1, the stroboscopic map can be written as

$$P_S = P_2 \circ ZDM \circ P_1,$$

where P_1 describes the evolution with flow Φ_1 through time t_1 and P_2 describes the Φ_1 through time $T - t_1$. The PDM may be preferable to use as an analytical tool for studying bifurcations of grazing limit cycles. It is also natural to apply the PDM for autonomous systems and the ZDM for time-periodically forced ones. The leading order terms of the ZDM and PDM generically have the same power, but the PDM correction takes non-zero time.

We do not give here the general forms of these maps. Unlike the case for transverse discontinuity mappings, there is no simple general expression valid for all cases of hybrid and piecewise-smooth systems. Indeed the detail evaluation of these mappings is rather lengthy in some cases; and forms the main thrust of Chapters 6, 7 and 8 in the cases of impacting hybrid systems, and piecewise-smooth systems with and without sliding, respectively. We shall also show in more detail how to combine the ZDM or PDM with the full flow of the system to produce an overall Poincaré mapand hence unfold the dynamics near a grazing limit cycle and other related DIBs.

2.6 Numerical methods

Many examples presented in this book rely on computations of orbits of piecewise-smooth and/or hybrid flows. For smooth flows, there are broadly speaking two classes of numerical methods for investigating the possible dynamics for a range of parameter values, namely: *direct numerical simulation*, and *numerical continuation* (also known as path-following). This classification also applies to piecewise-smooth systems. The rigorous numerical analysis of non-smooth dynamical systems remains a theory that is far from complete. Therefore, we shall take a practical approach in this book, since our goal is to use numerics to illustrate theory, rather than to analyze or derive optimal numerical algorithms.

2.6.1 Direct numerical simulation

When computing solutions to piecewise-smooth systems it is usually not possible to use general-purpose software packages directly, as most black-box numerical integration routines assume a high degree of smoothness of the solution. Accurate numerical computations must make special allowance for the non-smooth events that occur when a discontinuity boundary Σ_{ij} is crossed. Simulation methods for non-smooth systems fall broadly into two categories; *time-stepping* or *event-driven*. The former is most often used in many-particle rigid body dynamics written in complementarity form for which there can be perhaps millions of constraints and corresponding slack variables (Lagrange multipliers). For such problems, to accurately solve for *events* when one of the multipliers or constraint functions becomes zero within each time-step and to subsequently re-initiate the dynamics would be prohibitively computationally expensive. In contrast, the basic idea of time-stepping is to only check constraints at fixed times at intervals Δt. There are adaptations to standard methods for integrating ODEs and DAEs that are specifically designed for complementarity systems, some of which are based on linear complementarity problem solvers that have been developed in optimization theory. Clearly, errors are introduced by not accurately detecting the transition times, and therefore time-stepping schemes are often of low-order accuracy (i.e., with error estimates that $\sim O(\Delta t)^q$ for a low q) and can completely miss grazing events associated with low-velocity collisions. Several commercially available implementations of time-stepping algorithms are available, especially for the specific case of rigid body mechanics. These often have a variational formulation and are able to deal with the difficult problem of the collision of two rough bodies that may not have unique solutions. See the review by Brogliato and co-workers [41] and the Chapter by Abadie in [39, Ch. 2] for more details.

In this book we are largely concerned with low-dimensional systems with a small number of discontinuity boundaries (no more than say 10 of each). In that context, explicit *event-driven* schemes are feasible, fast and accurate. In these methods, trajectories within regions S_i are solved using standard numerical integration algorithms for smooth dynamical systems (e.g., Runge-Kutta, implicit solvers, etc.). Using these methods, the times at which a discontinuity boundary is hit are accurately solved for, and the problem is re-initialized there. Here we include the possibility of sliding or sticking flow by allowing portions $\tilde{\Sigma}_{ij}$ of discontinuity sets that are attracting to have the same status as open regions S_i, and to let the sliding vector field F_{ij} apply there. We then treat the boundary $\partial\tilde{\Sigma}$ as another discontinuity set. Similarly, in sticking regions for impact-hybrid systems, we can compute the explicit sticking flow that satisfies (2.43). Alternatively, one can use a DAE formulation, so that the Lagrange multipliers α or λ remain as part of the problem and a constraint $H_{ij} = 0$ is added which defines the discontinuity surface Σ_{ij}. There are now many reliable solvers for systems of differential algebraic equations, for example, DDASSL [218].

A key requirement for an event-driven method is the ability to define each discontinuity boundary as the zero set of a smooth function $H_{ij} = 0$. Also we have to carefully define a set of transition rules at each boundary that applies, if necessary, a reset rule R_{ij} and switches to the integration of a new dynamical system on the far side of the boundary. Thus, the time-integration of a trajectory of the dynamical system is reduced to the finding of a set of *event times* t_k and events $H_{ij}^{(k)}$ such that

$$H_{ij}^{(k)}(x(t_k)) = 0.$$

To achieve this we set up a series of *monitor functions*, the values of which are computed during each step of the time-integration. If one of these functions changes sign during a time step, then one needs to use a root finding method to accurately find where $H_{ij} = 0$. These ideas have been implemented in Matlab by Piiroinen & Kuznetsov [222].

Special care has to be taken to allow for the possibility of a sequence of event times converging onto a limit (for example, in a chattering sequence) followed by sticking or sliding. Clearly it is not appropriate to calculate all of the event times. To overcome this, it is typical to keep a record of the last few events. If it appears that the event times are converging to a limit, then this limit can be determined asymptotically, and then the procedure for a sliding or slicking solution applied; see [203] for details.

Let us now see how the event-driven method works specifically in the case of a two-zone Filippov system with sliding:

$$\dot{x} = \begin{cases} F_1(x), & \text{if} \quad H(x) > 0, \\ F_2(x), & \text{if} \quad H(x) < 0. \end{cases}$$

Note that the sliding vector field

$$F_s = (1-\alpha)F_1(x) + \alpha F_2(x), \quad \text{where} \quad \alpha = \frac{H_x F_1}{H_x F_1 - H_x F_2} \tag{2.80}$$

is defined in a full neighborhood of $\Sigma = \{H = 0\}$. The flow is such that $H_x \equiv 0$, so that it is confined to level sets $H = \text{const}$. So, a small error in initial condition $H(x(t_j)) = \varepsilon$ will not in theory lead to flow precisely on Σ but on another manifold a small distance away from it. In fact, as is well known from constrained time-integration [10], a numerical approximation to such flows will cause $H(x(t))$ to slowly drift away from this manifold. One resolution to this [222] is to replace the sliding vector field with a regularized version

$$\widehat{F}_s(x) = F_s - CH_x(x)H(x),$$

where C is a positive constant. Note that $\widehat{F}_{12} = F_{12}$ on Σ, but away from the switching manifold, we have exponential attraction in the direction H_x onto it. See Fig. 2.31.

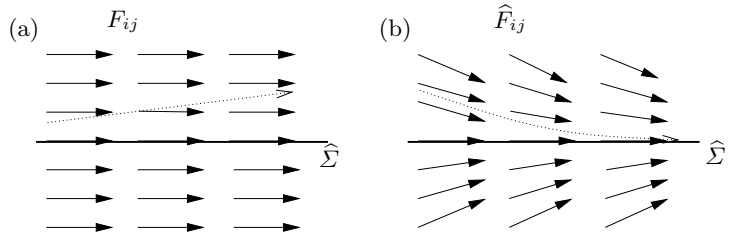

Fig. 2.31. (a) The sliding vector field F_{ij} and (b) the regularized version $\widehat{F}_{ij}$ near a discontinuity boundary Σ. Dashed lines indicate qualitatively what might happen to a numerical approximation to the flow.

One of the main uses of direct numerical simulation is to compute the bifurcation diagrams of the set of attracting solutions directly. In this process, for a fixed parameter value, a set of initial points is chosen and the flow from each point is determined. The flow is computed for a sufficiently long time for transients to decay and for the ensuing dynamics to be deemed to have converged onto an attractor. This dynamics is then recorded, perhaps in a suitable Poincaré section. The parameter is then changed slightly and the same process is repeated. Of course, one has to build up experience about the system in order to determine how long is a 'sufficiently long time'. However, an even more crucial question is to determine what set of initial conditions to take in order to converge to the various possible attractors. One approach here, which may minimize transient times, is to choose an initial condition for the new parameter value to be a point on the attractor at the previous parameter value. However, such an approach will necessarily miss the possibility of competing attractors present in the system. For example, consider the bifurcation diagram Fig. 1.26 for the DC–DC converter example, case study V, one sees several short intervals of the input voltage E for which in addition to the main bifurcation branch there are competing attractors (for example, a period-3 attractor around $E = 24$).

Thus, in general one should start from a range of different points within a suitably defined subset $\mathcal{D}$ of the phase space from which one has *a priori* knowledge that the attractors of the system must lie. But how to choose such points within this set? The number of points should of course be chosen to be as large as possible for the computational time available. One could start with a regular grid of points, but there are advantages in choosing the initial points at random. That is, at each fixed parameter value, use a *random* number generator to choose initial conditions in $\mathcal{D}$ uniformly. This way, the situation where attractors with small basins of attraction are missed consistently at each parameter value are likely to be avoided. We will refer to this method for computing bifurcation diagrams as a **Monte Carlo method**. Indeed, most of the bifurcation diagrams presented in this book were computed this way. The direct simulation method has many advantages in giving a quick and realistic

picture of the bifurcation diagram of a system without assuming any *a priori* structure about the number or form of the attractors.

2.6.2 Path-following

While having the merits described above, direct simulation suffers from the two disadvantages that it does not accurately pinpoint bifurcation points, and it only computes stable invariant sets (attractors). In order to accurately locate bifurcations it is sometimes necessary to compute *unstable* invariant sets. For example, the collision of a limit cycle with an unstable equilibrium can cause the sudden disappearance of that limit cycle; or, one might want to detect the presence of an unstable limit cycle that at some subsequent parameter value may re-stabilize at a fold. Hence there is a complimentary need for *direct methods* for computing specific invariant sets of dynamical systems. These typically comprise methods for numerical path-following of these solutions as a parameter varies, for detecting codimension-one bifurcations, and possibly continuation of these bifurcation points in two or more parameters. These bifurcations might be regular bifurcations that can also occur in smooth systems, or they might be DIBs associated with the changing of the event sequence of the orbit. For smooth systems, there is a large literature on such methods; see, for example, [168, Ch. 10] or [232] for general explanations, and for example the software AUTO [88] and MatCont [74].

Let us illustrate the key ideas applied to the continuation, as a single parameter μ varies, of fixed points of maps $x \to f(x, \mu)$. This will be equivalent, via the numerical construction of Poincaré maps, to the problem of finding periodic orbits of non-smooth systems that have a given event sequence. It is also entirely equivalent to computing equilibrium solutions of a piecewise-smooth system $\dot{x} = f(x, \mu)$ within some fixed region S_i. Once we can do this, then we can use event detection to find parameter values where the event sequence of the periodic orbit changes, or where a fixed point or equilibrium hits a switching set Σ_{ij}. Hence we naturally have a method for the detection of DIBs.

The general setting is to find paths in the parameter space of smooth parameterized systems of n equations in n unknowns that take the form

$$G(x, \mu) = 0, \qquad G : \mathbb{R}^n \times \mathbb{R}^1 \to \mathbb{R}^n, \tag{2.81}$$

given some initial solution $x = x_0$ at $\mu = \mu_0$. For example, when computing fixed points of maps, we take

$$G(x, \mu) = x - f(x, \mu).$$

The key idea behind numerical continuation is based on an appeal to the Implicit Function Theorem to compute sequences of points at small intervals along the solution curve $x(\mu) \approx \{(x_i, \mu_i), i = 0 \dots N\}$.

The most commonly used method for solving systems of nonlinear equations is Newton's method, but it is well known that this requires a sufficiently good initial guess in order to converge [153]. There are many modifications to the above method and implementation details. Its strength is the local *quadratic convergence* guaranteed by Newton's method. Its drawback is the requirement to know the Jacobian matrix G_x. This is particular problematical in the case of periodic orbits.

When computing a periodic orbit of a non-smooth system that involves the crossing of a discontinuity boundary, one essentially needs a method to compute the Poincaré map$P(x, \mu)$ from some section $\Pi := \{x : \pi(x) = 0\}$ to itself, see Fig. 2.26. This can be done via a *shooting method*. (For alternative ways of computing periodic orbits in Filippov systems via concatenating different boundary-value problems for each trajectory segment, see [72]). The shooting approach takes an initial condition in Π and solves the flow, through the various regions S_i back to Π again, taking a total time $\tau(x)$. This defines the point $P(x)$, and the function to which we apply the continuation algorithm is thus

$$G = x - P(x, \mu),$$

a zero of which represents the existence of a periodic orbit. Therefore the Jacobian we need is $G_x = I - P_x$, so we therefore need an expression for the linearized Poincaré mapP_x. Here it is useful to apply the discontinuity mapping Q described in the previous section. Indeed, for the case of transversal intersections, the saltation matrix correction has been used successfully for path-following [66] and for the detection of limit cycles [1].

So, now that we have the notation, definitions and methods (both analytical and numerical) at our disposal; we are ready to embark on a tour of different discontinuity-induced bifurcations. We start, in the next two chapters, with the case of maps.

http://www.springer.com/978-1-84628-039-9

Piecewise-smooth Dynamical Systems
Theory and Applications
Bernardo, M.; Budd, C.; Champneys, A.R.; Kowalczyk, P.
2008, XXII, 482 p., Hardcover
ISBN: 978-1-84628-039-9